THE SECONDARY COMPONENTS OF ALGOL SYSTEMS

M. PARTHASARATHY

Thesis submitted to the
Madurai University
for the Degree of
Doctor of Philosophy

INDIAN INSTITUTE OF ASTROPHYSICS

January 1979

Certificate from the Supervisor

I certify that the thesis entitled "THE SECONDARY COMPONENTS OF ALGOL SYSTEMS" by M. Parthasarathy is a record of the research carried out by him at the Indian Institute of Astrophysics. I declare that the thesis has not previously formed the basis for the award of any Degree, Diploma, Associateship, Fellowship or similar title. It contains an account of spectroscopic and photometric observations made by the candidate, of eclipsing binaries of the Algol type, and of his interpretation of the observed phenomena.

M K V Bappu

(M.K.V. Bappu)
Director
Indian Institute of Astrophysics

INDIAN INSTITUTE OF ASTROPHYSICS
BANGALORE-560034

Telephone: 41835
Telegrams: ASTRON

Certificate from the Supervisor

I certify that the Thesis entitled "THE SECONDARY COMPONENTS OF ALGOL SYSTEMS" by M. Parthasarathy is a record of the research carried out by him at the Indian Institute of Astrophysics. I declare that the thesis has not previously formed the basis for the award of any Degree, Diploma, Associateship, Fellowship or similar title. It contains an account of spectroscopic and photometric observations made by the candidate, of eclipsing binaries of the Algol type, and of his interpretation of the observed phenomena

M. K. V. Bappu
Director
Indian Institute of Astrophysics

given me this facility.

Thanks are due to Mr. A.V. Raveendran for his help in the reductions of the spectroscopic data of HU Tauri.

Mr. A.M. Batcha did the typing of the entire thesis. Mr. S. Muthukrishnan copied the diagrams in Indian Ink. Mr. R. Krishnamoorthy and Mr. Monnappa made the xerox copies of the diagrams. Mr. and Mrs. Krishnamoorthy did the bounding work of the thesis copies. My sincere thanks are due to each one of them for their timely help.

My thanks are due to all the technical staff members of the Indian Institute of Astrophysics in particular to Mr. A.T. Charles, Mr. R. Chandramohan, Mr. A. Sundareswaran, Mr. V. Chinnappan and Mr. F. Gabriel.

M. Parthasarathy

Bangalore-34
January 30, 1979

(M. Parthasarathy)

TABLE OF CONTENTS

TABLE OF CONTENTS

--

SUMMARY

In Algol-type close binary systems the primary is an early type main sequence star and the less massive secondary is typically a subgiant or giant of late spectral type. Algol-type systems present an evolutionary paradox, as the less massive star appears to be in an advanced stage of evolution, while the more massive companion is still on the main sequence. Crawford and Kopal suggested that the secondaries of typical Algol systems were originally the more massive components that had expanded to the critical limiting surface and then transferred much of their mass to the companion.

Until recently information on the secondary components has been obtained primarily from radial velocity and photometric studies.

Broad band and narrow band photometric studies have indicated ultraviolet excess for the secondaries. These have been interpreted by several observers in terms of metal deficiency. Narrow band photometry of the G band and the CN bands have also indicated metal deficiency for the secondaries. Until recently, no detailed abundance analysis of these objects has been made.

Analysis of the spectra of the secondary components in the blue-violet region have also indicated metal deficiency for the secondaries. Clearly, a detailed spectroscopic study of secondary components in Algol-type systems will shed light on the mass transfer event.

Reticon spectra of 1.9A resolution and in the red region, of the secondary components of U Cep (B7V + G8III) and U Sge (B8V + G5III) are analysed herein. A differential spectrum synthesis analysis of the spectrum of the secondary of U Cep relative to κ Gem (G8III) has been carried out. It is seen that the secondary component of U Cep has a normal composition with $[Fe/H] = 0.0 \pm 0.3$. Since U Cep is a result of Case A mass exchange (Paczynski 1971) the observed normal abundance of metals $[Fe/H] = 0.0 \pm 0.3$ and s-process elements in the secondary component is consistent with that expected from theories of evolution of close binary systems.

An analysis of the 1.8A resolution Reticon spectra of the secondary component of U Sge has also been carried out. A comparison of the U Sge secondary spectra to Gaussian broadened spectra of the standard stars has been made. A rotational velocity of 75 km/sec applied to the δ CrB (G5III), spectrum provided an excellent fit to the U Sge secondary spectrum. (The chemical composition of

δ CrB is normal). From comparison of U Sge secondary spectrum with the synthesized spectrum (T_{eff} = 5250K, log g = 3.0, [Fe/H] = 0.0) in the interval 6377 to 6409A, we find that metal abundance in the secondary component of U Sge is normal [Fe/H] = 0.0 $\pm$ 0.4.

Thus the secondary components of U Cep and U Sge have normal metal abundance. The observed mass ratios of U Cep and U Sge are q = 0.67 and 0.33 respectively. U Cep and U Sge are understood to have resulted from case A and case B mass exchange. The secondaries in these two systems have similar composition. These results indicate either that the mass transfer case A and case B do not lead to significant change in the chemical composition or that U Sge may not be a typical case B mass exchange system. Probably like U Cep, U Sge is also a result of case A mass exchange.

Infrared spectra of the secondary components of U Cep and U Sge have revealed another interesting aspect, which reflects their chromospheric activity. The CaII infrared triplet lines are found to be very weak in the spectrum of the secondary components of U Cep and U Sge. Weak CaII IR triplet lines are also noticed in σ Gem, a single lined spectroscopic binary with strong K line

emission. Enhanced chromospheric emission in the H and K lines seem to be accompanied by a weakening of the infrared absorption lines of CaII. The secondary components in U Cep and U Sge thus appear to have active chromospheres as a result of tidal effects.

Earlier investigators have interpreted the observed UV excess of the secondaries in terms of

i) metal deficiency of the secondary

ii) chromospheric activity of the secondary

iii) contamination of the colours of the secondary by light from an envelope surrounding the hot star that is not completely eclipsed at mid-primary minimum.

Since we find a normal chemical composition for the secondaries of U Cep and U Sge, the interpretation of observed UV excess in terms of metal deficiency is not valid.

From the observations of a recent outburst of U Cep, Batten has found variable UV excesses both within and outside eclipses. Thus the explanation that chromosphere activity as the source of UV excess is also not applicable.

The third possibility seems to be the more plausible one. There is a strong observational evidence for

circumstellar matter in Algol systems. From a photometric and spectroscopic study of HU Tau reported herein, we find the system to be that of the Algol-type with partial eclipses. Spectra obtained in the H_{α} region show evidence for presence of gas streams. From the derived dimensions of the system it is found that HU Tau is a semidetached system with a gas stream flowing from the secondary component to the primary.

CHAPTER 1

SOME ASPECTS OF ALGOL-TYPE SYSTEMS

1.1 Introduction

In Algol-type close binary systems, the more massive primary is an early type main sequence star and the less massive secondary is typically a subgiant or giant of late spectral type. Some of the well known, and to a certain extent well studied, systems of this type are Algol, U Cep, and U Sge. Algol-type systems present an evolutionary paradox since the less massive star appears to be in an advanced stage of evolution while the more massive companion is still on the main sequence. Crawford (1955) and Kopal (1955) suggested that the Algol type close binary systems have resulted from a large scale transfer of mass, as the secondary which was the more massive star in the original binary, evolved, filled its Roche lobe, and lost mass to the primary. Morton's (1960) fundamental paper confirmed Crawford's hypothesis of interchange of the components through a rapid mass exchange. Kippenhahn and Weigert (1967) were the first to calculate a sequence of models

describing the mass transfer phase. Kippenhahn and Weigert (1967) and Lauterborn (1970), proposed three different mass transfer cases, A, B and C, depending on whether mass transfer starts within the main sequence band, before the onset of helium burning, or after helium exhaustion. In recent years several excellent review articles on mass transfer and evolution of close binary systems were written by Kopal (1971), Paczynski (1971), Plavec (1968, 1970, 1973).

Our knowledge of the secondaries in the Algol-type systems is obtained from an analysis of the radial velocity curves and light curves. One can usually determine the radial velocity curve of the primary component only, because, of the great disparity in brightness between the two stars. Because of this disparity in brightnese, the secondary minima in the UBV light curves of these systems are very shallow. Secondary minima of significant depth can be obtained by observing these systems in the infrared. This is indeed seen in the infrared light curves of Algol (Chen and Reuning (1966), Nadeau et al. (1978), RW Mon (Brukalska et al. 1969), RW Tau (Bookmyer 1977) and U Cep (Khozov and Minaev 1969). Since the secondary minimum in the infrared is relatively deeper, analysis

of the infrared light curves will give us accurate system parameters and it is also possible to study the surface brightness distribution of the subgiant secondary component which is distorted on account of axial rotation and tidal action (cf. Budding and Kopal (1970) and Parthasarathy (1972)). Successful efforts to detect the secondary components in Algol type systems by Popper (1973), Tomkin (1978), Tomkin and Lambert (1978), and Tomkin (1979) have resulted in accurate system parameters for AS Eri, δ Lib, Algol and U Sge respectively. Another important aspect to understand evolutionary process of Algol type close binary systems is to determine the chemical composition of the primary and secondary components. Miner (1966) utilized narrow band photometry and found moderate-to-extreme metal deficiency for a dozen subgiant secondaries in Algol type systems. Only recently has an abundance analysis for the secondaries been attempted from high dispersion spectra by Naftilan (1976) and Parthasarathy, Lambert and Tomkin (1979).

1.2 Observed Properties of Algol-type close binary systems

a) Period Variations

Most of the Algol-type systems display from time to time rapid and almost discontinuous changes of the

period. U Cep, U Sge and RW Tau are typical examples of systems showing sudden period changes. O-C diagrams of Kreiner (1971) and Frieboes - Conde and Herczeg (1973) show that periods of Algol systems increase and decrease randomly by $\Delta P/P = 10^{-5}$. From an analysis of the times of minima of a large number of close binary systems, Wood (1950) indicated that the systems with secondaries near the limits of dynamical stability show strong tendency to irregular variations of period. These sudden changes of period always speak in favour of ejection of material from the subgiant. Transfer of mass from the subgiant secondary to the massive primary under stationary conditions leads to an increase in the orbital period. The only stationary process that can account for a decrease in period is loss of mass from the system with sufficient loss of angular momentum. Bierman and Hall (1973) propose that, for the Algol-type systems, continuous non-stationary exchange of angular momentum between orbit and rotation is the reason for the alternate period changes. Bierman and Hall's (1973) model is based on the assumption that sudden bursts of mass are transferred to the hot star as a result of Bath (1972) type instability. The mass and the angular momentum thus lost from the cooler star is stored temporarily as rotation in the surface layers of the hotter star,

or onto a disc around the hotter star thereby decreasing the orbital period, and then goes back into orbit as increased turbulence "lets the friction time scale catch up with the dynamical time scale of the mass transfer thereby increasing the period". Recently, Hall (1975) summarized the problem of period changes caused by mass loss or mass transfer. Batten et al. (1975) and Plavec and Polidan (1975) have detected an outburst in U Cep. From an analysis of O-C diagrams of U Cep, Biermann and Hall (1973), Hall (1977) and Bakos and Tremko (1977) indicate that the outbursts are accompanied by sudden period changes. Biermann and Hall (1973) while proposing the above described model predict that the light during totality should slant up when the period is decreasing and not when it is increasing. Such a slant in totality is found in U Cep Batten (1974), RW Tau Grant (1959) (see Figure 1) and in several other Algol-type systems.

b) Light Changes during totality

Many Algol-type systems show marked asymmetries in their light variations. Quite often one finds that the shoulder of the light curve near the first contact is fainter than the shoulder at the fourth contact. There is also a slight increase in brightness immediately after the primary minimum. In U Cep the light curve near

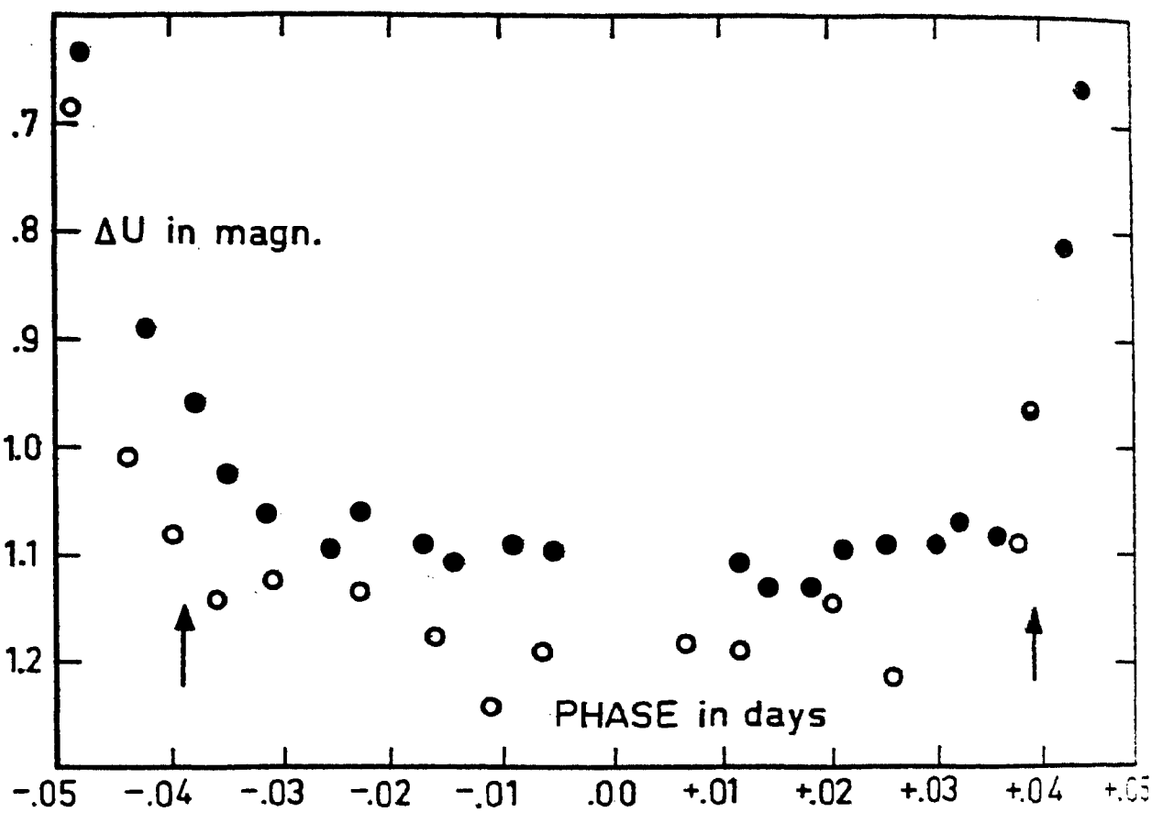

Fig. 1a. The bottom of primary eclipse of U Cep in ultraviolet light. The arrows indicate the position to second and third contact. Open circles and fitted circles are Hall's (1974) February 1970 and April 1970 observations respectively.

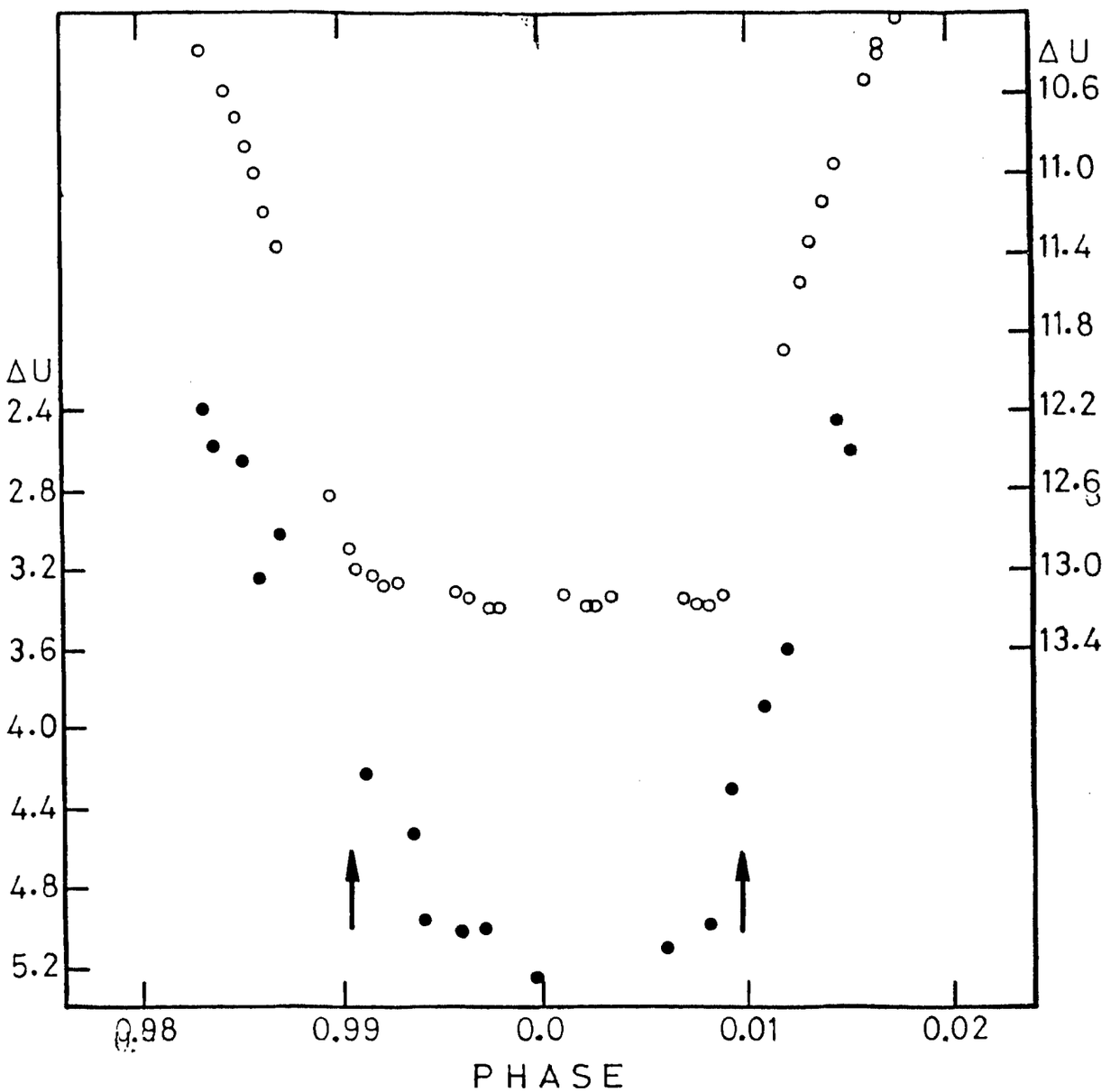

Fig.1b. The bottom of primary eclipse of RW Tauri in ultraviolet light. The arrows indicate the position of second and third contact. Filled circles represent the 1968 observations of Bookmayer (1977) and open circles represent the 1955 observations of Grant (1959).

the first contact is fainter than at the fourth contact. Bolkadze (1956) suggested that the asymmetry of the light curve is due to the veiling of the light of the primary star by the gas stream. More pronounced asymmetries in the light variations near the second and third contact are noticed in U Cep, U Sge, RW Tau and SW Cyg. The duration of totality is also found to be variable and wavelength dependent in a few systems. In RW Tau, Grant (1959) found on some nights near the beginning of totality, systematic deviations of $0^m.02$, $0^m.05$ and $0^m.1$ in V, B and U respectively, as compared with the remainder of the minimum. This residual light is found to be due to the gaseous ring observed spectroscopically by Joy (1942). Recently Bookmyer (1977) from her UBVRI photometry of RW Tau found the system to be somewhat brighter before mid-eclipse than after mid-eclipse. In Figure 1b the observations of RW Tau by Grant (1959) and Bookmyer (1977) near the total phase of the primary minimum are plotted. It is evident that the shape and duration of totality have changed from the time of Grant's (1959) observations. It is not known, how frequent are these changes. At times the minima are found to be symmetrical and almost constant in light during the totality. Recent observations of U Cep by Olson (1974) and Hall (1975) indicate that variations take

place during the total phase from cycle to cycle. In Figure 1a, the U observations of U Cep made by Hall (1975) on 26-27 February 1970 and 2-3 April 1970 are shown. Batten (1974) and Hall and Walter (1974) found evidence for a flattened disk around the primary component of U Cep. Hall and Walter (1974) examined 104 light curves obtained between 1880 and 1970. They defined a quantity Δ m as the difference of brightness at the beginning and at the end of totality. Thus, the light at totality slants up when Δ m is positive and slants down when it is negative. They find that the abrupt period changes are correlated with positive values of Δm. However, the ultraviolet Δm determinations show a different trend. The correlation between epochs of period decrease and Δm can be explained by a combination of two effects. Hall and Garrison (1972) had suggested that the upward slant during totality is due to accumulation of luminous matter, which has been ejected from the subgiant, passing around the B star, and concentrated in front of its leading hemisphere. While explaining the cause for alternate period changes of Algol systems, Bierman and Hall (1973) propose that the gas stream should have maximum strength during the time when the period is decreasing. Sudden period changes, slanted totalities and variable ultraviolet

excesses during the totality seems to be a common feature of Algol-type systems.

c) Masses and Luminosities

The massive components in the Algol-type (semi-detached) systems are on or near the main sequence. They seem to obey the mass luminosity relation fairly well. The secondary components have filled their Roche lobes, are above the main sequence, and are subgiants and giants of later spectral type. The mass of the subgiant secondary in a few systems (AS Eri, DN Ori, TY Peg etc.) is only about 0.2 $M_\odot$. The subgiant components are overluminous. The luminosity excess is defined as the difference in bolometric magnitude between the subgiant and a main sequence star with the same mass. Ziolkowski (1969) computed the luminosity excess of subgiant secondary components in 39 Algol-type systems. The excess in luminosity is found to be correlated with the observed mass ratio. There is a clear tendency for the luminosity excess to increase with decreasing mass of the secondary. In more massive binaries with total mass 5 $M_\odot$ or more the luminosity excess is found to be not larger than 3^m. In systems with smaller mass (short period Algol-type systems) luminosity excesses of upto 10^m have been found. Paczynski (1967) and Gianuone et al. (1968) suggested that

the observed semi-detached low mass binaries correspond to case B mass exchange. On the basis of the distribution of the observed luminosity excesses Ziolkowski (1969) suggested that they are the result of mass exchange case AB. However, this explanation requires small central hydrogen content at the beginning of the mass transfer or large scale mass loss from the system.

d) Circumstellar Matter

Batten (1970, 1973a, and 1973b), and Sahade and Wood (1978) have reviewed various aspects of circumstellar matter in close binary systems. Spectroscopic studies of several systems have revealed the existence of gaseous stream flow from the subgiant secondaries and a circumstellar disk or an envelope around the massive primary component and in some cases an extended outer envelope. From the spectroscopic observations of RW Tau, Joy (1947) discovered emission lines in the eclipse spectrum of RW Tau and also the variation in intensity from one eclipse to another. Joy interpreted the eclipse spectrum of RW Tau by postulating that the B9 primary is surrounded by a gaseous ring.

Struve and Sahade (1957) found red displaced emission line at 0.25 phase. Sahade (1958) and Andrews (1967)

studiend it in detail and found the corresponding feature at 0.75 phase to be much weaker with no hydrogen line emission seen in the eclipse spectrum. The emission feature appears to arise in the stream between the two stars. Struve, Sahade and Huang (1957) have also suggested that emission from the gaseous stream between the two stars is partly responsible for the apparent line doubling observed in the spectrum of U CrB at quadratures. Batten and Laskarides (1969) have attempted to explain in the same way the distorted line profile in the spectrum of U Cep at quadratures. More recently Batten et al. (1975) and Plavec and Polidan (1975) detected an outburst of U Cep. They found emission in all Balmer lines from H_α to H_{18} and also in the H and K lines of CaII, λ 4481 of MgII and possibly in some lines of FeII and HeI. The emission persisted for about 40 days and is found to arise in a disk around the primary star. Some of the characteristics noticed during this outburst by Batten et al (1975), Plavec and Polidan (1975), Olson (1976) and Rhombs and Fix (1977) are:

1. H_α emission was accompanied by a sharp absorption component, which was also seen at H_β, H_γ and H_δ with a displacement to the violet corresponding to velocity of several hundred kms^{-1}.

2. Asymmetric primary minimum and shortened duration of totality. Duration of totality in U is found to be relatively much shorter.

3. UV excess within and outside the eclipses. UV excess during the primary minimum was found to be variable.

e) <u>The Ultraviolet Excess and Metallicity</u>

Ultraviolet excess have been observed in the subgiants of many Algol-type eclipsing binaries. Systems showing UV excess are listed in Table 1. The UV excess values listed are taken from Devinney et al (1970), Koch (1972), Hall et al (1972), McNamara (1967) and McNamara and Feltz (1976). For single stars the δ(U-B) is an indicator of metal abundance (Wallerstein 1962). This interpretation, which is valid for a single star, has been extended by several observers to explain the observed UV excess of the subgiant secondaries in terms of metal deficiency. The δ(U-B) values given in Table 1 indicate that the UV excess is large for systems with longer orbital periods. Such large negative values are not definitely due to abundance anomalies. For late type dwarfs an abundance of $[Fe/H] = -1.0$ produces an UV excess of δ(U-B) = 0.2 (Wallerstein 1962). In several

Table 1

Intrinsic colours and UV excesses of the secondary components

	Period (days)	Spectral type	$(B-V)_o$	$(U-B)_o$	(U-B)
R CMa	1.14	F1V G4IV	+1.14	+0.68	-0.39
W UMi	1.70	A3 K0IV	+1.15	-0.02	-1.04
U Cep	2.49	B7V G8III	+0.88	+0.40	-0.17
RW Tau	2.77	B8 K0IV	+1.00	+0.91	-0.09
WW Cyg	3.32	B7V G8IV	+0.82	+0.48	-0.1
U Sge	3.38	B8.5IV-V G2-5III-IV	(+0.46)	(+0.40)	-0.15
SW Cyg	4.57	A2e K0	+1.16	+1.0	-0.27
WW Dra	4.63	G5V G5	+0.97	+0.63	-0.12
TU Mon	5.05	B5V F0III	+0.31	+0.04	-0.04
AX Mon	5.90	A5III-IV G2III	+0.73	+0.20	-0.07
S Vel	5.93	A5V K5III	+1.05	+0.78	-0.12
RS Cep	12.42	A5e G			-0.6
RW Per	13.20	A5 gG0	+0.90	+0.15	-0.47
SX Cas	36.57	A6e gG6	+0.92	-0.05	-0.71
AU Cyg	38.44	gF4 K5III	+1.30	+0.06	-0.81
RZ Oph	261.94	F3Ib K5Ib	+1.5	+1.2	-0.6

systems the observed UV excess is much larger than what can be interpreted in terms of metal deficiency of the secondaries. There seems to be a dependence of δ(U-B) for the secondaries on log P (Koch 1972). The observed UV excess of the secondaries listed in Table 1, when plotted against the separation between the components (log a) indicates the existance of a possible linear relationship. Thus the apparent UV excess of the secondaries probably is not due to the metal deficiency. Probably the circumstellar envelope around the hot star or around the whole system is contaminating the colours of the secondaries. From the photometric study of SW Cyg Hall (1972) came to the conclusion that the observed UV excess in SW Cyg and in other Algol-type systems is due to contamination by light from an envelope surrounding the hot star that is not completely eclipsed at mid-primary minimum.

Very few attempts have been made to study Algol-secondaries employing narrow bandpass filters. Miner (1966) utilized narrow band photometry to study a dozen Algol systems. Spectral features measured by him were the G-band, the CN bands at 4200A and a metallic abundance index $\Delta m'$. Miner found metal deficiency for all twelve. From the correlation of $\Delta m'$ index (Miner 1966) with

[Fe/H], Hall (1967) (also see Koch 1972) found the average [Fe/H] for the twelve secondaries to be -0.96. McNamara (1967) and McNamara and Felts (1976) from uvby photometry found [Fe/H] = -0.9 and -0.6 for the secondary components of U Cep and U Sge respectively. Similar metal deficiencies were reported by Hall (1967) who measured the CN index defined by Griffin and Redman (1960). Hall (1967) found CN to be deficient by a factor of 3, this result was confirmed by Spinrad and Taylor (1959) from scanner observations of AR Lacertae. Sistero (1968, 1971) found ultraviolet excess in the subgiant secondary component of S Vel and interpreted it in terms of metal deficiency. Bond (1972) obtained an ultraviolet spectrogram of S Vel during the totality and found the spectrum to be very much similar to that of δ Lep a high-velocity red giant, and reached to the conclusion that the secondary component of S Vel is metal deficient. Naftilan (1975) finds slight metal deficiency in three Algol systems. However, Batten et al. (1973) and Rhombs and Fix (1977) detected an increased ultraviolet excess within and outside the eclipses of U Cep during the 1974 outburst. Thus the interpretation of the observed ultraviolet excess of the subgiant secondaries in terms of metal deficiency seems to be improper.

According to current understanding the subgiant secondaries in Algol-type systems are in the stage of post main sequence evolution. And it is generally accepted that they have lost considerable mass to the current primary. Thus knowledge of the chemical compesition of the primary and secondary components will enable us to understand the evolution of these interesting systems. My interest to study the problem of ultraviolet excess and metallicity of the subgiant secondaries came after I found a flare type H α emission in HU Tau (see Figure 2) on a 17A/mm dispersion spectrum plate taken on 3rd January 1974 with the 1.0 meter telescope of the Kavalur Observatory. Subsequently Batten et al. (1975) and Plavec and Polidan (1975) reported an outburst in U Cep and found an increased ultraviolet excess within and outside the eclipses.

From spectroscopic and photometric study of HU Tau, it is found that it is a typical Algol system with partial eclipses. Uncontaminated spectra of the subgiant secondaries can be obtained only during the total phase of the primary eclipse and, therefore, it is not possible to get such an uncontaminated spectrum of the subgiant secondary in HU Tau. Since the duration of totality is short and the secondary is faint, the

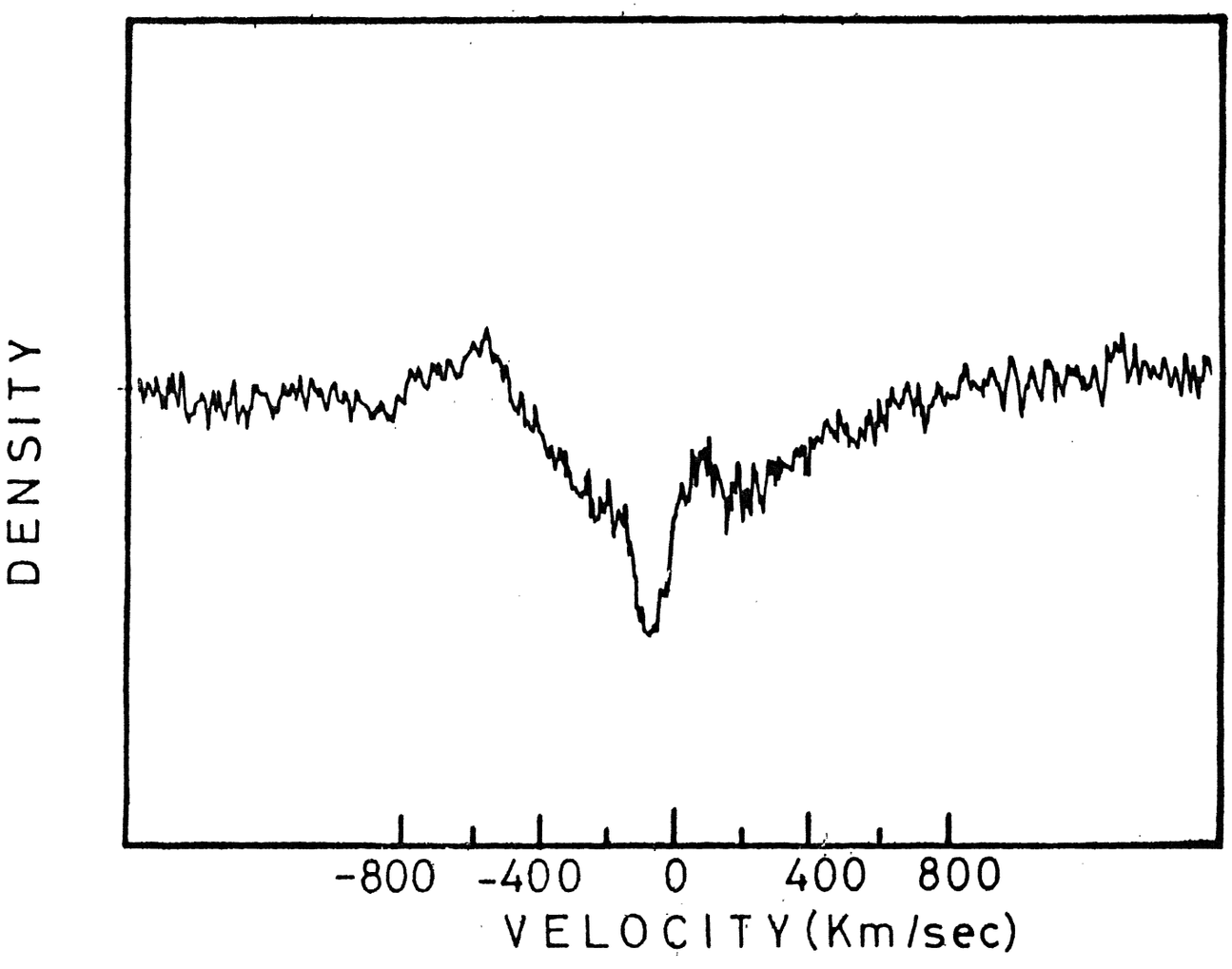

Fig.2. Microphotometer tracing of the line profile of Hα on January 3, 1974. The zero of the velocity scale is the rest position of Hα line. Violet is at the left.

acquisition of spectra of the necessary high quality is a challenge to high quantum efficiency detectors. U Cep and U Sge, which at minimum light have V magnitude 9.1 and 9.2 respectively, are the two brightest Algol systems with total primary eclipses. In the next few chapters, an analysis of the spectra of the secondary components of U Cep and U Sge are presented, followed by a derivation of the parameters of the typical Algol system HU Tau.

CHAPTER 2

THE CHEMICAL COMPOSITION OF SECONDARY COMPONENTS ALGOL-TYPE SYSTEMS

2.1 Introduction

Until recently, information on the secondary components of Algol type systems has been obtained primarily from radial velocity and photometric studies. Broad band photometry has indicated large ultraviolet excess for the secondaries (Table 1). A few narrow band photometric studies (Miner 1966, Hall 1967) have also indicated that the secondary components of Algol systems are metal-poor. The Algol-type systems originate from a large scale transfer of mass when the secondary, which was the more massive star in the original binary, evolved filled its Roche lobe and lost mass to the primary Crawford (1955), Kopal (1955). Only recently has an abundance analysis for the secondaries been attempted from high dispersion spectra. Naftilan (1976) used spectrum synthesis and curve of growth approaches to analyse the spectrum of the secondary of U Sge. Spectra in the interval 3500Å to 4800Å showed a mild metal deficiency ($[Fe/H] = -0.7$) for the iron group and similar

elements and a slight enhancement for some s-process elements. This is an interesting result which, if confirmed and extended to other Algol systems, surely places severe constraints on the mass transfer models.

The secondary components in Algol type systems are generally subgiants or giants of late spectral type and they are rotating synchronously. For this reason, the rotational velocities of these stars are very high compared to the single stars of similar spectral type. Therefore, the spectra show severe rotational broadening so that normally strong lines are broad and shallow. The line blending and continuum level uncertainty associated with the crowded spectra of G and K stars are both enhanced by the rotational line broadening. These difficulties are minimized by working with red and near infrared spectra. Uncontaminated spectra of the secondary can be obtained only in the total phase of the primary eclipse. Systems like HU Tau with partial eclipses are not suited for this purpose. Since the duration of totality is short and the secondary is faint, the acquisition of spectra of the necessary high quality is a very difficult task with conventional techniques. With modern digital detectors like the Reticon Silicon diode array, it is possible to get high quality spectra even

for fainter stars within a short exposure time. The two brightest of the totally eclipsing Algol systems are U Cep and U Sge, which at minimum light have V magnitudes 9.1 and 9.2 respectively. This analysis is confined to the study of high dispersion spectra of these two objects.

2.2 The Observations

Spectra of the secondaries of U Cep and U Sge were obtained with the 2.7m telescope and Tull coude spectrometer equipped with a Reticon Silicon diode array detector (Vogt, Tull and Kelton 1978). The spectra of U Cep were obtained near zero phase of the primary eclipse. Single exposures covering 430A were obtained at a resolution of 1.9A with 0.46A per diode. With an exposure time of about fifty minutes in average seeing the unsmoothed spectra have a signal to noise ratio of about 80. Each exposure was centered near mid-eclipse and had a duration much shorter than the duration of totality, so that the secondary spectrum was obtained without contamination from the light of the primary. The spectra were centered at 6200A, 6320A and at 8620A. The spectrum centered at 8620A includes the CaII infrared triplet lines at 8498A, 8542A and 8662A. These regions were selected because examination of the Arcturus spectrum

(Griffin 1968) suggested that they contained an useful mixture of moderately strong lines and broad continuum regions.

The spectra of U Sge were also obtained at the middle of primary eclipse. The 6320A region spectrum was obtained by Prof. David Lambert and Dr. Jos Tomkin on 22nd June 1978. The length of the spectrum is 210A and the resolution is 1.8A with 0.23A per diode. The unsmoothed spectrum has a signal to noise ratio of about 113. An additional spectrum, which was centered at 8620A which includes CaII infrared triplet lines was obtained by Dr. Jos Tomkin on 29th July 1977. The resolution is 1.8A and the length of the spectrum is 430A with 0.46A per diode. Instrumental resolution of 1.9A and 1.8A for U Cep and U Sge respectively were chosen to match the anticipated rotational broadening. Some of the details of the spectra are given below.

Year	Time of mid exposure	Phase	Wavelength at the center	Length of the spectrum	Å/ diode	Resolution
			U Cep			
1977	Dec 2.1063	0.010	6200A	430A	0.46A	1.9A
1978	Feb 22.3243	0.997	6320A	430A	0.46A	1.9A
1977	Jul 25.4410	0.008	8620A	430A	0.46A	1.9A
			U Sge			
1977	Jul 29.360	0.997	8620A	430A	0.46A	1.8A
1978	Jun 22.292	0.000	6320A	210A	0.23A	1.8A

The spectra of U Cep on 2nd December 1977 and 22nd February 1977 were obtained by Prof. David Lambert, Dr. Jos Tomkin and myself. Rest of the spectra were obtained by Prof. David Lambert and Dr. Jos Tomkin and Dr. Jos Tomkin. Spectra were also obtained of several standard stars: δ CrB (G5III), κ Gem (G8III), β Gem (KoIII) and γ Cyg (KoIV). The lines in the spectra of the standard stars, which were observed at the same resolution, are sharper than in U Cep and U Sge (see Figures 3, 5, and 6). This demonstrates that the resolution is sufficiently high and the broadening of the U Cep spectra is mostly rotational and not instrumental.

2.3 The Rotational Velocity of the Secondary component of U Cep

Batten (1974) has recently given a new unified interpretation of U Cep. The spectral types of the primary and secondary components are B7V and G8III-IV. The orbital period of the system is very nearly equal to 2.5 days. The duration of total phase is nearly two hours. The duration of totality is found to be variable. The various parameters of the system are given in Table 2.

Table 13 2

Physical parameters of U Cep and U Sge

	U Cep		U Sge	
	Primary	Secondary	Primary	Secondary
Period (days	2.49		3.38	
Separation ($R_\odot$)	14.7		18.6	
Mass Ratio	0.67		0.33	
Spectral type	B7V	G8III	B8.5IV-V	G2-5III-IV
Mass ($M_\odot$)	4.2	2.8	5.7	1.9
Radius ($R_\odot$)	2.9	4.8	4.2	5.6
Roche radius ($R_\odot$)	6.1	5.1	8.9	5.3
M_V	-0.2	+2.5	-0.4	+2.2
log g	4.14	3.32	3.95	3.22
V_{syn} (km/sec)	58.9	97.5	62.9	83.8
V_{rot} (km/sec)	200-300		76	

In the spectrum synthesis approach to an abundance analysis, the line broadening resulting from the rotation of the secondary must be taken into account. The orbital period and stellar radius of 4.8 $R_\odot$ (Batten (1974) and Cester et al. (1977)) correspond to a predicted equatorial rotational velocity of 97 ± 10 km s^{-1} on the assumption that the secondary is rotating synchronously. To check this prediction, we have matched the U Cep secondary spectra to Gaussian broadened spectra of the standard stars. The broadening velocity, V_G, of the Gaussian velocity distribution, $\exp(-(V/V_G)^2)$, is related to the rotational velocity by $V_G = \frac{2}{3} V_{Rot} \sin i$ (Unsold and Struve, 1949). A rotational velocity of 90 ± 8 km s^{-1} (V_G = 60 km s^{-1}) applied to the κ Gem spectrum provides an excellent fit to the U Cep secondary spectrum (Figure 3). The spectral type of κ Gem is G8III and matches the classification of the secondary of U Cep (Batten 1974). The rotational velocity solution is not sensitive to the choice of standard star. The result shows that the secondary is rotating synchronously.

2.4 The Chemical Composition of the Secondary component of U Cep

Since the spectrum of the secondary is so severely broadened by rotation, a spectrum synthesis approach is

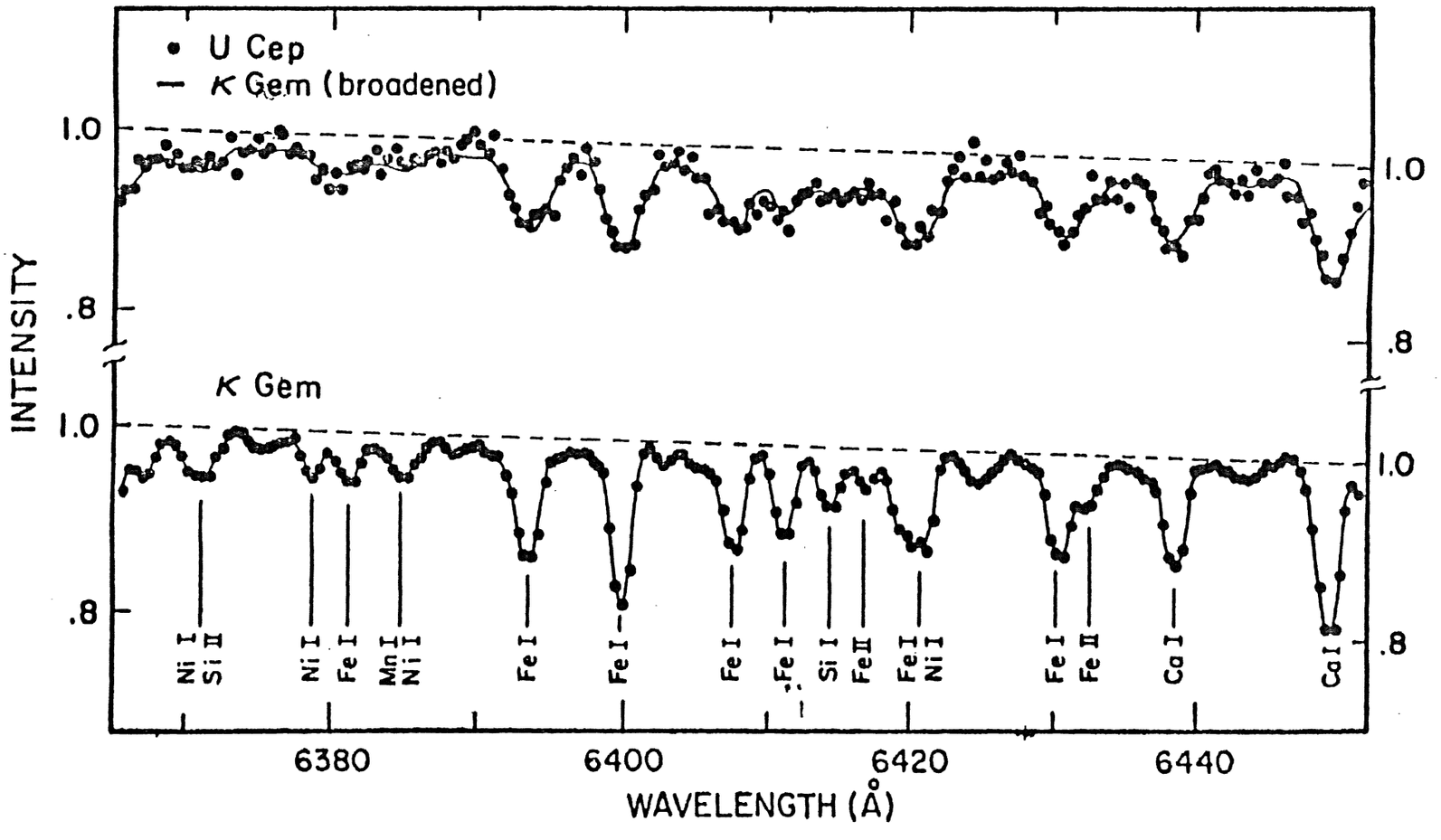

Fig. 3 . Spectra of κ Gem and the secondary component of U Cep.

especially attractive. Our analysis was done in two stages. The standard star κ Gem is a close match to the U Cep secondary. For κ Gem, Williams (1971) obtained the basic parameters T_{eff} = 4990 K and log g = 2.9. The composition of κ Gem appears to be solar (Burbidge and Burbidge 1957; Williams 1971; Hansen and Kjaergaard 1971). Colour indices and the spectral type suggest T_{eff} = 5000 K for the U Cep secondary (Batten 1974). Cester et al. (1977) from light curve synthesis obtained T_{eff} = 5080 K. The known mass and radius (Batten 1974) provide log g = 3.5 $\pm$ 0.2.

Since the neutral metal lines are relatively insensitive to small differences in the surface gravity, our initial analysis took the observed κ Gem spectrum and broadened it by the predicted amount for synchronous rotation. The fit to the observed U Cep secondary spectrum was excellent (Figure 3). Clearly, large abundance differences between U Cep and κ Gem are excluded by this direct test.

In order to obtain a quantitative understanding of the abundance similarity, we undertook to account for the difference in gravity between κ Gem and the U Cep secondary. A model atmosphere with T_{eff} = 5000 K, log g = 3.0 and solar composition was taken from the grid

constructed by Bell et al. (1976). We synthesized two spectrum intervals: 6139.0 to 6158.5Å and 6377 to 6409Å. An initial line selection was made using the Kurucz and Peytreman (1975) table. A total microturbulent velocity of 2 km s^{-1} was adopted with a macroturbulence of 4 km s^{-1}. The computed spectrum was convolved with the instrumental profile. Through adjustment of the oscillator strengths, the synthetic spectrum was forced to match the observed spectrum of κ Gem. In the next step, we retained the revised oscillator strengths and recomputed the spectrum for model atmospheres T_{eff} = 5250 K, log g = 3.75, T_{eff} = 5250 K, log g = 3.0, T_{eff} = 5000 K, log g = 3.0 (the κ Gem model), and three different input abundances, solar, one-third solar and one-tenth solar. To match the U cep spectra, the synthetic spectra were rotationally broadened. The calculations with 3 different models enable us to assess the effect of reasonable temperature and surface gravity uncertainties on the synthetic spectra. Observed and synthetic spectra in the wavelength interval 6377 to 6409Å are compared in Figure 4. The spectrum computed for solar abundances for model atmosphere T_{eff} = 5000, log g = 3.0 is a good fit. It is clear that with the other two models the solar abundance synthetic spectra also provide the best fit.

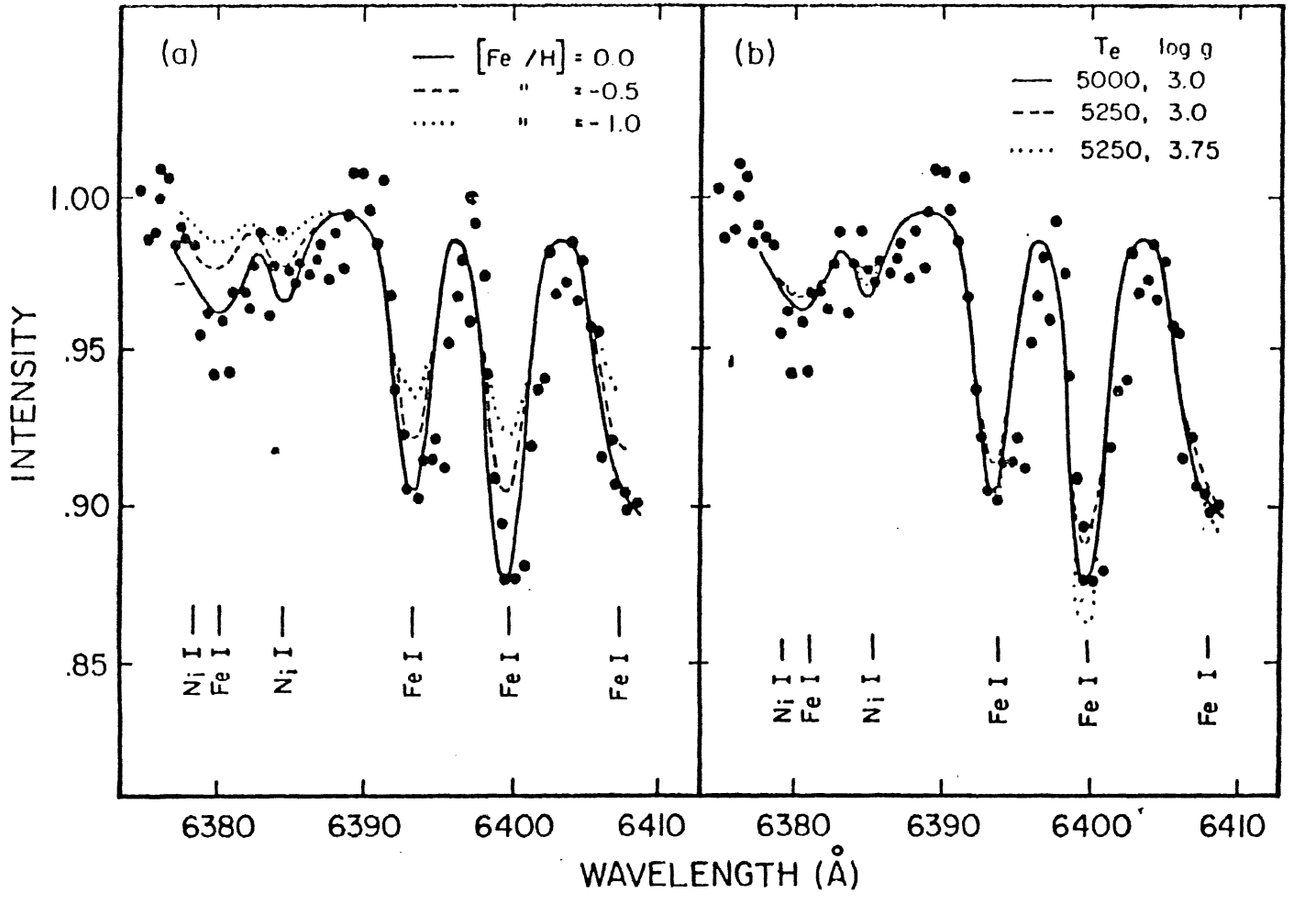

Fig. 4 . The spectrum of the secondary component of U Cep between 6380 and 6410Å. The synthetic spectra in (a) show the effect of a decrease in the adopted metal abundance; a model atmosphere T_e = 5000 K and log g = 3.0 was adopted. Synthetic spectra in (b) show the sensitivity of the synthetic spectra to changes in the adopted effective temperature (T_e) and surface gravity (log g); they were computed with solar metal abundances.

Since the rotational broadening is so severe, the shallow lines in the U Cep secondary spectrum correspond to deep saturated lines in the K Gem spectrum. Hence, their conversion to a metal abundance is subject to modest uncertainty. Inspection of the synthetic spectra suggests that $[Fe/H] = 0.0 \pm 0.3$ where the uncertainty includes a contribution from the T_{eff} and log g uncertainties. Our results are in agreement with Baldwin (1973) who, from a spectral comparison of the secondary of U Cep with single stars of the same spectral type, also found no evidence of significant metal deficiency. They exclude the metal deficiency, $[Fe/H] = -0.9$ (McNamara 1967), obtained from narrow band photometry.

The majority of the lines belong to metals in the range Na to the iron group. The Ba II line at 6141.7Å is included and appears to correspond to a solar abundance. Therefore, we suggest that the s-process elements also have a solar abundance. This contrasts with Naftilan's (1976) results for the U Sge secondary where he reported a metal deficiency but an s-process over-abundance.

Our analysis of the U Cep secondary spectrum is clear evidence for normal abundances of iron peak elements. We, therefore, conclude that the interpretation, of the UV

excess obtained from the broad band and narrow band photometry as an indicator of metal abundance, is invalid. The cause of the UV excess could be due to circumstellar gas.

Rhombs and Fix (1976, 1977) made flux measurements of U Cep during totality and also outside the eclipse covering the wavelength interval 3300Å to 5900Å, with a bandpass of 30Å. They found that a large UV excess seen during totality in 1974 was absent in 1975. Similar results were reported by Batten et al. (1975) and Olson (1976). If a similar UV excess affected the photometric observations of the secondary of U Cep, it would provide an explanation of the discrepant photometric metal abundances. The Rhombs and Fix measurements of the secondary of U Cep show the excess UV flux increases steeply shortward of 4000Å. There is no significant excess flux at longer wavelengths. Excess flux with this distribution will affect the u band (central wavelength 3500Å) but not the v, b, and y bands (central wavelengths 4110, 4670 and 5470Å, respectively). The $[Fe/H]$ of -0.9, estimated by McNamara (1967) for the secondary of U Cep, is based on the difference between its m_1 index (which is independent of u) and the m_1 indices of stars in the same location of a c_1 versus b-y diagram. The c_1 index depends directly on

μ and, therefore, may provide a misleading location in the c_1 versus b-y diagram and, thence, a misleading estimate of the metal abundance. We note, however, that the observations of Rhombs and Fix were made during the "outburst-mass transfer activity", a rare event described by Batten et al. (1975) and Plavec and Polidan (1975). If the photometry was done during a quiescent phase, when the UV excess was greatly reduced, then an alternative explanation of the discrepancy between the photometric and spectroscopic abundances must be sought.

2.5 Analysis of the Spectra of the Secondary Component of U Sge

U Sge is another interesting Algol-type close binary system. The orbital period of the system is 3.38 days. The duration of totality is 112 minutes. The spectral types of the primary and secondary components are B8.5 IV-V and G2-5 III-IV (Cester and Pucillo (1972) and McNamara and Feltz (1976)). The physical parameters of the system are given in Table 2. Recently Tomkin (1979) determined the velocity curve of the secondary of U Sge. The mass ratio and masses of the primary and secondary determined by him are: $m_2/m_1 = 0.33$, $m_1 = 5.7\ m_\odot$ and $m_2 = 1.9\ m_\odot$ respectively. Thus the system parameters are now known accurately. The mass ratio of U Cep is 0.67

and that of U Sge is 0.33. Plavec (1973) suggests that the U Sge system has resulted from case B mass exchange. Recently Naftilan (1976) found mild metal deficiency $[Fe/H] = -0.7$ for the secondary component of U Sge from an analysis of the spectra in the interval 3500A to 4800A. McNamara and Feltz from uvby photometry also concluded that the secondary component is metal deficient. Cester et al. (1977) from light curve synthesis obtained $T_{eff} = 5350$ K for the secondary. The mass and radius of the secondary (Table 2) provide log g = 3.2. The computed rotational velocity V_{syn} is found to be 83.8 km/sec.

The McDonald spectrum of U Sge was obtained at the middle of primary eclipse on 22nd June 1978.

The resolution is 1.8Å with 0.23A/diode. The unsmoothed spectrum has a signal to noise ratio of 113. From the orbital period and radius of the secondary (Table 2) the calculated synchronous rotational velocity is 83.8 km/sec. To check this we have matched the U Sge secondary 6320A region spectrum and 8620A region spectrum to Gaussian broadened spectra of the standard stars. This method has already been described in the section on the rotational velocity of the secondary component of U Cep. A rotational velocity of 75 km s^{-1} (V_G = 50 km s^{-1}) applied to the CrI spectrum provides a good fit to the

U Sge secondary spectrum (Figures 5 and 6). The broadened spectrum of δ CrB is a close fit to the spectrum of the secondary component of U Sge. While the FeI lines match well there are slight deviations noticed in the region of TiI lines near 6260A. However, the spectrum interval 6250A to 6260A matches very well with the broadened spectral region of δ CrB. This feature is a blend of FeI, SiI, NiI and TiI lines (Figure 5). Similarly the spectral region near 6245A which is a blend of SiI, ScI and FeI lines matches perfectly with the broadened spectrum of δ CrB (Figure 5). A similar close fit is seen in the interval 6315A to 6350A. The feature of 6318A is a blend of CaI, MgI and FeI lines and the feature at 6343A is a blend of FeI and CaI lines. These two regions match very well with the broadened spectrum of δ CrB. Similarly the broadened spectrum of δ CrB (G5III) also matches very well with the spectrum of the secondary component of U Sge in the wavelength interval 8400A to 8800A. Since the abundance of elements in δ CrB is normal $[Fe/H] = 0.0$, and since the broadened spectrum of δ CrB matches very well with the spectrum of the secondary component of U Sge, one can conclude that the U Sge secondary is not metal deficient. Naftilan (1976) has reported a moderate metal deficiency ($[Fe/H] = -0.7$) in U Sge secondary from an analysis of its spectrum in the region 3500A to 4800A, with also a

slight enhancement of s-process elements. Since the temperatures and gravities of the secondary components of U Cep and U Sge are comparable (see Table 2), we can compare synthesized spectra given in Figure 4. The closest model satisfying the temperature and gravity of U Sge secondary is T_e = 5250 K and log g = 3.0 (see Figure 4 and Table 2). Comparison of the observed spectrum of the U Sge secondary in the wavelength interval 6377 to 6409A with the synthesized spectrum in that region with T_e = 5250 K and log g = 3.0 (dashed line in Figure 4). We find no evidence for metal deficiency. The synthesized spectrum matches well with the observed spectrum of U Sge secondary. From the synthesized spectra it is clear that a metal deficiency of $[Fe/H] = -0.5$ produces significant deviations even in the case of strong lines when compared with a spectrum synthesized with normal metal abundances.

From the above discussion we can conclude that the secondary of U Sge is not metal deficient. However, a detailed curve of growth and spectrum synthesis analysis in the red is essential to narrow down the uncertainties.

The interpretation of observed UV excess of the secondary components in Algol-type close binary systems in terms of metal deficiency is not valid. McNamara and

Peltz (1976) from uvby photometry found [Fe/H] = -0.6 for the secondary component of U Sge. McNamara and Peltz (1976) from uvby photometry of U Sge found more ultraviolet radiation near the beginning of totality than at the end of totality. They also found that the observed times of light minima were delayed by 43 seconds in u relative to the observed light minima inferred from the v, b and y observations. Oster and Pucillo (1972) also found that the length of totality appeared to be somewhat shorter in U than in B and V. This excess radiation must be a superposition of Balmer continuum radiation from the gas stream or disk on the radiation of the G2 star. A similar phenomenon was noticed in U Cep and RW Tau (see Figure 1a and 1b) and SW Cyg (Hall and Garrison 1972). The duration of totality in these three systems is shorter in U than in B and V. Hall and Garrison (1972) interpreted the observed UV excess in SW Cyg in terms of contamination of the colours of the secondary component by light from an envelope surrounding the hot star that is not completely eclipsed at mid-primary minimum.

CHAPTER 3

CHROMOSPHERIC ACTIVITY OF ALGOL SECONDARIES

Observational details of the infrared spectra of the secondaries of U Cep and U Sge in the region of the CaII triplet lines are given in Chapter 2.

From Figure 7, we notice that the CaII infrared triplet lines are weak in the secondaries of U Cep and U Sge relative to their intensities in standard stars. In comparing the spectra, the standard star spectra are broadened by the predicted rotational velocities. More observations are needed to confirm our suspicion that the CaII lines are weaker than the standards in all Algol secondaries.

In normal stars, the cores of the CaII lines (and the H and K lines) are formed in the chromosphere. The H and K line emission intensity is found to be an indicator of chromospheric activity (Wilson and Bappu 1957, Wilson 1963). Since the H and K lines and the infrared triplet share a common upper state, enhanced chromospheric emission in the H and K lines is likely to be accompanied by a weakening of the infrared absorption lines. Baldwin (1973) reported that the CaII K line in the spectrum of the

secondary of U Cep appears to be filled in by emission. The H and K lines of CaII are also found to be in emission and are of high intensity in the spectrum of the secondary component of S Vel (Bond 1972).

The correlation between strong H and K emission and weaker absorption lines of CaII infrared triplet may well be found in other binaries with a late type giant component. An example is δ^- Gem (K1 III, P = 19.6 days) which is a single lined spectroscopic binary with K line emission intensity of 5 on the scale of Wilson and Bappu (1957) and Wilson (1976). Our infrared spectrum of δ^- Gem shows that the triplet lines are weaker than in a standard star of similar spectral type. Attribution of the CaII effects to enhanced chromospheric activity is confirmed by the detection of a strong HeI 10830A line in δ^- Gem (Zirin 1976).

Shine and Linsky (1972) have studied the CaII lines in the active and quiet regions of the sun. In plage regions, the infrared CaII lines are weak relative to the line profiles obtained in the quiet regions. In a weak plage, the 8498A line, the least opaque of the triplet lines, shows a definite double reversal. The cores of all lines show reversals in the bright lines. Differences between quiet and plage regions are attributed to larger

chromospheric temperature gradients and the resulting increase in electron density in plage regions.

The secondary components of U Cep and U Sge have filled their Roche lobes and the tides raised by their massive companions seem to increase the chromospheric heating. An analysis of intensities of CaII emission K line in spectroscopic binaries is made by Glebocki and Stawikowski (1977) and Young and Koniges (1977) and Evans (1977). They find a correlation between K line emission intensity and orbital period. Their results indicate that the tidal forces can change structure of the chromospheres in late type giants. If we extend this analogy to the secondary components of Algol systems, the tidal forces on the secondary by the massive hot companion are enormous. Further observations of Algol secondaries in the region of H and K lines and infrared triplet lines of CaII are needed to study their chromospheric activity.

In conclusion, we note that there is a very significant amount of calcium chromospheric emission in the secondaries of the Algol-type systems as shown by the CaII infrared triplet. Such high chromospheric intensities in a "quiet" state implies chromospheric

emission originating from agencies caused by the convection zone in the star (Bappu and Sivaraman 1971) that are vastly amplified by tidal distortion.

CHAPTER 4

AN ANALYSIS OF THE LIGHT AND VELOCITY CURVES

The light variability of HU Tauri ($5^{m}.7$, B9V) was discovered by Strohmeier (1960). Mammano et al. (1967) found it to be a single lined spectroscopic binary and determined the spectroscopic orbital elements. Because of its brightness, short period, early spectral type and the possibility of total eclipse (Mammano et al. 1967), I decided to study the system photoelectrically and spectroscopically.

4.1 Photometric elements of HU Tauri

Photometric observations of HU Tauri were made with the 38cm refractor telescope of the Nizamiah Observatory on 24 nights during January 1971 - January 1973, using the standard B and V filters a GR1230A DC amplifier and Brown recorder. HR 1472 and HR 1479 were used as the comparison and check stars respectively (see Table 3). A total of 638 blue and 453 yellow observations were obtained. All the observations were corrected for atmospheric extinction using the nightly atmospheric extenction coefficients

Table 2

Variable and comparison stars data

		V	B-V	U-B	Spectral type
Variable	HU Tau	5.70	-0.06	-0.37	B9V
Comparison	HR 1472	5.79	+0.31	+0.06	A8V
Check	HR 1479	4.68	+0.16	+0.15	A5V

determined from the observations of the comparison star. After applying the extinction corrections the extra atmospheric magnitude differences Δ m (variable star - comparison star) in blue and yellow were obtained. In Table 5a and 5b the heliocentric Julian day of observation and Δm_b and Δm_v are listed. The variation in the observed magnitude differences between the comparison and check stars on different nights is found to be $\pm$ $0^m.015$. UBV standard stars were observed on three nights during February 1971-January 1973. After correcting for atmospheric extinction the standard star observations were used to determine the magnitude and colour transformation coefficients by least squares method. The extra atmospheric magnitudes and colours of the standard stars, and the magnitude and colour transformation coefficients are given in Table 4. The differential magnitudes (variable - comparison) listed in Table 5a and 5b are on the instrumental system.

4.2 Times of Minima and Period

From the photometric observations listed in Table 5a and 5b four times of primary minimum and two times of secondary minimum of HU Tau are determined and are listed in Table 6. On the basis of photographic observations, Strohmeier and Knigge (1960) determined the following

	V	B-V	Sp	1971 Feb.28.8UT		1973 Jan.4.9UT		1973 Jan.5.9UT	
				v	b-v	v	b-v	v	b-v
L CMa	4.36	-0.07	B3II	-1.595	-1.011	-1.176	-0.918	-1.022	-0.892
β Cnc	3.52	+1.48	K4III	-2.329	+0.032	-	-	-	-
ρ Gem	4.16	+0.32	F0V	-1.812	-0.708	-1.383	-0.639	-1.251	-0.626
φ Gem	4.95	+0.10	A3V	-1.000	-0.874	-0.620	-0.794	-0.473	-0.763
τ_1 Hya	4.30	-0.19	B3V	-1.666	-1.103	-1.345	-1.015	-1.177	-0.994
40 Leo	4.83	+0.44	F6IV	-1.139	-0.628	-0.776	-0.540	-0.604	-0.539
11 LMi	5.41	+0.77	G8IV	-	-	-0.132	-0.320	0.029	-0.296
+4°1414	5.91	-0.02	B0III	-	-	+0.299	-0.897	0.495	-0.879

Magnitude and Colour transformation coefficients

	ϵ_v	ζ_v	μ_{bv}	ζ_{bv}
1971 Feb. 28	-0.068	5.967	1.478	1.404
	±0.013	±0.083	±0.027	±0.022
1973 Jan. 4	-0.057	5.590	1.372	1.197
	±0.034	±0.012	±0.014	±0.010
1973 Jan. 5	-0.047	5.427	1.387	1.181
	±0.026	±0.010	±0.018	±0.013

Table 5a

Yellow Observations of HU Tauri

S.No.	JD(hel) 2440000+	Δm_v
1	1010.1044	0.633
2	1010.1067	0.641
3	1010.1162	0.497
4	1010.1200	0.477
5	1010.1280	0.479
6	1010.1314	0.451
7	1010.1438	0.339
8	1010.1470	0.299
9	1010.1555	0.260
10	1010.1578	0.239
11	1010.1678	0.199
12	1010.1706	0.161
13	1010.1963	0.090
14	1010.1988	0.090
15	1010.2071	0.096
16	1010.2095	0.102
17	1010.2335	0.091
18	1010.2356	0.085
19	1010.2547	0.089
20	1010.2571	0.056
21	1010.2439	0.085
22	1010.2464	0.088
23	1011.0910	0.092
24	1011.0953	0.106
25	1011.0965	0.105
26	1011.1073	0.105
27	1011.1106	0.106
28	1011.1226	0.098
29	1011.1237	0.102
30	1011.1358	0.079
31	1011.1372	0.079
32	1011.1486	0.054
33	1011.1497	0.062
34	1011.1638	0.067
35	1011.1650	0.071
36	1011.1771	0.063
37	1011.1778	0.073
38	1011.1789	0.080
39	1011.1903	0.044
40	1011.1917	0.021
41	1011.2035	0.038
42	1011.2042	0.039
43	1011.2157	0.065
44	1011.2164	0.062
45	1011.2275	0.073
46	1011.2282	0.062
47	1012.0802	0.739
48	1012.0833	0.774
49	1012.0850	0.784
50	1012.0922	0.789
51	1012.0929	0.819
52	1012.0958	0.835
53	1012.0970	0.853
54	1012.1038	0.853
55	1012.1045	0.860
56	1012.1051	0.869
57	1012.1058	0.881
58	1012.1104	0.890
59	1012.1190	0.873
60	1012.1251	0.857
61	1012.1274	0.870
62	1012.1288	0.852
63	1012.1371	0.809
64	1012.1382	0.806
65	1012.1465	0.804
66	1012.1486	0.774
67	1012.1583	0.678
68	1012.1593	0.671
69	1012.1677	0.597
70	1012.1708	0.535
71	1012.1808	0.433
72	1012.1833	0.427
73	1012.1951	0.375
74	1012.1972	0.365
75	1012.2049	0.319
76	1012.2072	0.305
77	1013.0765	0.070
78	1013.0782	0.057
79	1013.0889	0.071
80	1013.1001	0.141
81	1013.1126	0.127
82	1013.1154	0.103
83	1013.1216	0.118
84	1013.1237	0.129
85	1013.1291	0.154
86	1013.1321	0.089
87	1013.1615	0.077
88	1013.1633	0.092
89	1013.1726	0.044
90	1013.1744	0.034
91	1014.0870	0.355
92	1014.0777	0.397
93	1014.0984	0.466
94	1014.0990	0.483
95	1014.1107	0.576
96	1014.1114	0.586
97	1014.1176	0.638
98	1014.1183	0.635
99	1016.0948	0.100
100	1016.0962	0.106
101	1016.1037	0.143
102	1016.1056	0.162
103	1262.2081	0.038
104	1262.2193	0.042
105	1262.2275	0.071
106	1262.2568	0.040
107	1262.2623	0.035
108	1262.2706	0.035
109	1262.2706	0.033
110	1262.2789	0.034
111	1262.2845	0.060
112	1262.2882	0.047
113	1269.3523	0.044
114	1269.3662	0.078
115	1269.3766	0.064
116	1269.3989	0.042
117	1269.4072	0.013
118	1269.4148	0.071
119	1269.4218	0.017
120	1269.4280	0.007
121	1269.4357	0.073
122	1274.1947	0.052
123	1274.1966	0.091
124	1274.2047	0.099
125	1274.2084	0.079
126	1274.2107	0.110
127	1274.2187	0.081
128	1274.2209	0.116
129	1274.2306	0.073
130	1274.2306	0.077
131	1274.2433	0.103
132	1274.2442	0.116
133	1274.2651	0.096
134	1274.2658	0.103
135	1274.2791	0.100
136	1274.2805	0.134
137	1274.2820	0.123
138	1275.1628	0.113
139	1275.1640	0.114
140	1275.1754	0.114
141	1275.1761	0.128
142	1275.1867	0.143
143	1275.1878	0.150
144	1275.1992	0.237
145	1275.1999	0.240
146	1275.2151	0.284
147	1275.2157	0.300
148	1275.2255	0.337
149	1275.2264	0.356
150	1275.2360	0.431
151	1275.2367	0.453
152	1275.2478	0.505
153	1275.2484	0.545
154	1275.2595	0.631
155	1275.2599	0.666
156	1275.2692	0.716
157	1275.2699	0.727
158	1275.2799	0.780
159	1275.2807	0.789
160	1275.2854	0.815
161	1275.2855	0.824
162	1275.2980	0.845
163	1275.2987	0.867
164	1275.3031	0.870
165	1275.3038	0.878
166	1275.3264	0.835
167	1275.3275	0.841
168	1275.3375	0.815
169	1275.3382	0.814
170	1275.3446	0.774
171	1275.3446	0.732
172	1275.3563	0.674
173	1275.3570	0.694

Table 5a - continued

S.No.	JD(hel) 2440000+	Δm_v
174	1272.3916	0.337
175	1275.3679	0.560
176	1275.3774	0.494
177	1275.3783	0.486
178	1275.3889	0.391
179	1275.3894	0.388
180	1275.4005	0.303
181	1275.4017	0.307
182	1275.4172	0.193
183	1275.4182	0.206
184	1275.4189	0.188
185	1275.4321	0.135
186	1275.4328	0.140
187	1275.4500	0.105
188	1275.4505	0.114
189	1275.4615	0.091
190	1275.4622	0.107
191	1275.4714	0.099
192	1275.4721	0.097
193	1295.1594	0.029
194	1295.1602	0.011
195	1295.1701	0.067
196	1295.1782	0.044
197	1295.1789	0.050
198	1295.1893	0.058
199	1295.1903	0.113
200	1295.2018	0.058
201	1295.2025	0.056
202	1295.2186	0.043
203	1295.2194	0.066
204	1295.2292	0.048
205	1295.2309	0.046
206	1295.2652	0.055
207	1295.2671	0.060
208	1295.2678	0.054
209	1295.2768	0.052
210	1295.2775	0.052
211	1295.2873	0.049
212	1295.2879	0.047
213	1295.2999	0.024
214	1295.3007	0.028
215	1295.3150	0.035
216	1295.3157	0.033
217	1295.3294	0.024
218	1295.3301	0.024
219	1295.3397	0.055
220	1295.3405	0.051
221	1295.3514	0.028
222	1295.3521	0.019
223	1295.3811	0.058
224	1295.3818	0.060
225	1295.3912	0.100
226	1295.3920	0.057
227	1295.4018	0.030
228	1295.4027	0.036
229	1295.4141	0.049
230	1295.4146	0.040
231	1295.4255	0.047
232	1295.4262	0.043
233	1349.1783	0.135
234	1349.1867	0.204
235	1349.1891	0.072
236	1349.1952	0.104
237	1349.1976	0.132
238	1349.2047	0.081
239	1349.2075	0.184
240	1349.2141	0.112
241	1349.2174	0.034
242	1349.2261	0.211
243	1349.2342	0.221
244	1349.2371	0.295
245	1349.2483	0.295
246	1349.2506	0.362
247	1349.2580	0.381
248	1349.2611	0.374
249	1349.2681	0.499
250	1349.2696	0.509
251	1349.2726	0.535
252	1349.2830	0.572
253	1349.2839	0.557
254	1349.2939	0.627
255	1349.2954	0.657
256	1349.3050	0.809
257	1349.3059	0.782
258	1687.1145	0.037
259	1687.1298	0.053
260	1687.1326	0.043

S.No.	JD(hel) 2440000+	Δm_v
261	1687.1417	0.030
262	1687.1441	0.022
263	1687.2545	0.018
264	1687.2576	0.025
265	1687.2691	0.024
266	1687.2715	0.023
267	1687.2759	0.013
268	1687.2820	0.006
269	1687.2859	0.042
270	1687.2920	0.046
271	1687.3004	0.050
272	1687.3031	0.045
273	1687.3115	0.056
274	1687.3139	0.053
275	1687.3213	0.044
276	1687.3234	0.036
277	1687.3366	0.025
278	1687.3431	0.032
279	1687.1110	0.034
280	1688.1062	0.015
281	1688.1076	0.006
282	1688.1152	0.032
283	1688.1214	0.045
284	1688.1374	0.037
285	1688.1443	0.032
286	1688.1516	0.020
287	1688.1585	0.017
288	1688.1692	0.026
289	1688.1764	0.046
290	1688.2395	0.062
291	1688.2454	0.076
292	1688.2513	0.092
293	1688.2572	0.063
294	1688.2631	0.044
295	1688.2858	0.045
296	1688.2914	0.068
297	1688.2973	0.065
298	1688.3024	0.070
299	1688.3080	0.074
300	1688.3132	0.045
301	1688.3191	0.050
302	1694.1266	0.032
303	1694.1290	0.042
304	1694.1360	0.057
305	1694.1439	0.045
306	1694.1508	0.041
307	1694.1597	0.043
308	1694.1895	0.035
309	1694.1990	0.027
310	1694.2064	0.017
311	1694.2277	0.034
312	1694.2336	0.052
313	1694.2409	0.048
314	1694.2470	0.053
315	1694.2531	0.066
316	1694.2585	0.026
317	1694.2640	0.018
318	1694.2696	0.018
319	1694.2756	0.040
320	1694.2836	0.044
321	1694.2904	0.050
322	1694.2965	0.045
323	1694.3037	0.045
324	1694.3100	0.046
325	1694.3171	0.061
326	1694.3294	0.065
327	1694.3362	0.049
328	1702.1215	0.055
329	1702.1244	0.061
330	1702.1322	0.059
331	1702.1645	0.062
332	1702.1728	0.037
333	1702.1827	0.027
334	1702.2026	0.068
335	1702.2090	0.041
336	1702.2160	0.033
337	1702.2234	0.070
338	1702.2341	0.040
339	1702.2489	0.043
340	1702.2593	0.048
341	1702.2658	0.042
342	1702.2722	0.036
343	1702.2781	0.051
344	1702.2836	0.052
345	1702.2902	0.057
346	1702.2966	0.069
347	1702.3041	0.069

Table 3a - continued

S.No.	JD(hel) 2440000+	Δm_v
348	1704.2085	0.054
349	1704.2109	0.052
35C	1704.2184	C.058
351	1704.2209	0.065
352	1704.2281	0.045
353	1704.2304	0.065
354	1704.2367	0.043
355	1704.2387	0.051
356	1704.2451	0.053
357	1704.2607	0.072
358	1704.2776	0.032
359	1704.2839	C.029
36C	1704.2916	0.054
361	1704.2972	C.061
362	1704.3033	0.049
363	1704.3092	0.040
364	1704.3165	0.052
365	1705.1159	0.832
366	1705.1184	0.792
367	1705.1246	0.742
368	1705.1541	0.588
369	1705.1607	0.463
37C	1705.1631	0.434
371	1705.1685	0.445
372	1705.1751	0.356
373	1705.1781	C.334
374	1705.1857	0.325
375	1705.1937	0.251
376	1705.2289	0.099
377	1705.2348	0.083
378	1705.2413	0.070
379	1705.2560	0.072
38C	1705.2615	C.047
381	1705.2671	0.086
382	1705.2781	0.082
383	1705.2830	0.085
384	1705.2883	C.091
385	1705.2989	0.089
386	1705.3045	0.068
387	1705.3100	0.081
388	1706.0972	0.107
389	1706.1006	0.086
39C	1706.1074	0.082
391	1706.1099	0.092
392	1706.1167	0.120
393	1706.1238	0.091
394	1706.1523	0.096
395	1706.1588	0.100
396	1706.1657	C.093
397	1706.1717	0.096
398	1706.1799	0.082
399	1706.1854	0.065
4CC	1706.1910	C.064
4C1	1706.1969	0.084
4C2	1706.2020	0.087
4C3	1706.2125	C.097
4C4	1706.2187	0.054
4C5	1706.2299	0.049
4C6	1706.3368	0.057
4C7	1706.2430	0.060
4C8	1706.2483	0.055
4C9	1706.2534	0.035
41C	1706.2581	0.035
411	1706.2631	0.040
412	1706.2681	0.055
413	1706.2731	0.044
414	1706.2789	0.050
415	1706.2877	C.041
416	1706.2930	0.028
417	1706.2985	0.039
418	1706.3034	0.029
419	1707.1132	0.729
42C	1707.1224	0.809
421	1707.1484	0.845
422	1707.1559	0.869
423	1707.1634	0.838
424	1707.1693	0.841
425	1707.1981	0.633
426	1707.2000	0.604
427	1707.2066	0.545
428	1707.2118	0.505
429	1707.2167	0.451
43C	1707.2218	0.440
431	1707.2273	0.379
432	1707.2329	0.342
433	1708.1117	0.146
434	1708.1453	C.075
435	1708.1522	0.087

S.No.	JD(hel) 2440000+	Δm_v
436	1708.1596	0.124
437	1708.1624	0.103
438	1708.1675	0.116
439	1708.1737	0.079
44C	1708.1796	0.087
441	1708.1857	C.074
442	1708.1914	0.110
443	1708.1964	0.109
444	1708.2015	0.103
445	1708.2189	C.086
446	1708.2223	0.152
447	1708.2234	0.140
448	1708.2501	0.075
449	1708.2547	0.063
45C	1708.2744	0.067
451	1708.2814	0.077
452	1708.2864	0.080
453	1708.2964	0.021

Table 5b

Blue observations of HU Tauri

S.No.	JD(hel) 2440000+	Δm_b	S.No.	JD(hel) 2440000+	Δm_b
			87	983.2725	0.446
			88	983.2794	0.502
1	981.1456	-0.086	89	983.2808	0.520
2	981.1463	-0.086	90	983.2822	0.536
3	981.1473	-0.086	91	983.2826	0.569
4	981.1644	0.013	92	983.2882	0.545
5	981.1658	0.008	93	983.2889	0.568
6	981.1702	0.030	94	983.2899	0.552
7	981.1709	0.084	95	983.2947	0.597
8	981.1760	0.078	96	983.2951	0.596
9	981.1764	0.086	97	983.2961	0.634
10	981.1822	0.149	98	983.2972	0.629
11	981.1829	0.167	99	983.3021	0.650
12	981.1840	0.172	100	983.3024	0.648
13	981.1951	0.205			
14	981.1958	0.315			
15	981.1965	0.321	101	983.3037	0.655
16	981.1975	0.324	102	983.3090	0.683
17	981.2034	0.304	103	983.3097	0.683
18	981.2041	0.326	104	983.3111	0.683
19	981.2048	0.326	105	983.3118	0.707
20	981.2104	0.413	106	983.3232	0.710
			107	983.3239	0.717
			108	983.3246	0.705
21	981.2107	0.414	109	983.3294	0.608
22	981.2280	0.539	110	983.3298	0.677
23	981.2359	0.621	111	983.3301	0.706
24	981.2405	0.643	112	983.3308	0.638
25	981.2565	0.680	113	1010.1193	0.280
26	981.2576	0.678	114	1010.1290	0.249
27	981.2621	0.679	115	1010.1301	0.232
28	981.2625	0.678	116	1010.1447	0.099
29	981.2732	0.623	117	1010.1451	0.095
30	981.2736	0.615	118	1010.1460	0.081
31	981.2778	0.634	119	1010.1562	0.016
32	981.2784	0.631	120	1010.1569	0.015
33	981.2824	0.632			
34	981.2829	0.631			
35	981.2875	0.593	121	1010.1693	-0.052
36	981.2878	0.587	122	1010.1700	-0.058
37	981.2954	0.626	123	1010.1976	-0.157
38	981.2958	0.624	124	1010.1981	-0.165
39	981.2996	0.552	125	1010.2080	-0.166
40	981.3000	0.550	126	1010.2087	-0.148
			127	1010.2342	-0.129
			128	1010.2349	-0.144
41	981.3049	0.493	129	1010.2446	-0.125
42	981.3053	0.492	130	1010.2453	-0.121
43	981.3114	0.461	131	1010.2553	-0.138
44	981.3118	0.458	132	1010.2557	-0.120
45	981.3173	0.393	133	1010.1057	0.392
46	981.3176	0.409	134	1010.1075	0.390
47	983.1500	-0.110	135	1010.1172	0.296
48	983.1514	-0.088	136	1010.1179	0.283
49	983.1524	-0.092	137	1011.0930	-0.184
50	983.1597	-0.131	138	1011.0941	-0.187
51	983.1607	-0.143	139	1011.1087	-0.171
52	983.1666	-0.170	140	1011.1094	-0.165
53	983.1680	-0.165			
54	983.1687	-0.173			
55	983.1743	-0.163	141	1011.1247	-0.188
56	983.1750	-0.161	142	1011.1258	-0.197
57	983.1919	-0.125	143	1011.1382	-0.170
58	983.1926	-0.135	144	1011.1393	-0.151
59	983.1989	-0.123	145	1011.1511	-0.192
60	983.1999	-0.117	146	1011.1525	-0.189
			147	1011.1532	-0.193
			148	1011.1664	-0.180
61	983.1954	-0.111	149	1011.1671	-0.186
62	983.1961	-0.111	150	1011.1759	-0.176
63	983.2010	-0.104	151	1011.1809	-0.180
64	983.2017	-0.099	152	1011.1930	-0.223
65	983.2028	-0.094	153	1011.1941	-0.213
66	983.2071	-0.069	154	1011.2055	-0.172
67	983.2079	-0.053	155	1011.2066	-0.184
68	983.2187	0.0	156	1011.2174	-0.177
69	983.2194	-0.008	157	1011.2180	-0.166
70	983.2253	0.065	158	1011.2289	-0.130
71	983.2260	0.067	159	1011.2296	-0.139
72	983.2322	0.108	160	1012.0819	0.549
73	983.2326	0.103			
74	983.2378	0.131			
75	983.2382	0.130	161	1012.0841	0.576
76	983.2392	0.167	162	1012.0938	0.652
77	983.2399	0.148	163	1012.0947	0.664
78	983.2461	0.214	164	1012.1065	0.692
79	983.2472	0.215	165	1012.1076	0.690
80	983.2521	0.258	166	1012.1086	0.705
			167	1012.1093	0.710
			168	1012.1201	0.667
81	983.2528	0.263	169	1012.1259	0.668
82	983.2676	0.366	170	1012.1281	0.657
83	983.2687	0.389	171	1012.1299	0.651
84	983.2694	0.381	172	1012.1392	0.587
85	983.2711	0.425	173	1012.1399	0.572
86	983.2718	0.431	174	1012.1475	0.522

Table 5b - continued

S.No.	JD(hel) 2440000+	Δm_b	S.No.	JD(hel) 2440000+	Δm_b
175	1014.1498	0.330	261	1270.3010	-0.202
176	1012.1604	0.416	262	1270.3018	-0.153
177	1012.1612	0.401	263	1270.3071	-0.204
178	1012.1694	0.368	264	1270.3076	-0.211
179	1012.1722	0.318	265	1270.3571	-0.201
180	1012.1819	0.177	266	1270.3586	-0.202
			267	1270.3661	-0.201
181	1012.1826	0.194	268	1270.3669	-0.219
182	1012.1859	0.141	269	1270.3725	-0.181
183	1012.1961	0.135	270	1270.3738	-0.188
184	1012.1982	0.128	271	1270.3793	-0.162
185	1012.2058	0.046	272	1270.3800	-0.163
186	1012.2083	0.038	273	1270.3856	-0.212
187	1012.2160	-0.002	274	1270.3865	-0.194
188	1012.2183	-0.011	275	1270.3875	-0.215
189	1012.2285	0.002	276	1270.3923	-0.207
190	1012.2306	-0.053	277	1270.3930	-0.207
191	1013.0772	-0.198	278	1270.3974	-0.194
192	1013.0789	-0.169	279	1270.3979	-0.187
193	1013.0890	-0.220	280	1270.4020	-0.215
194	1013.1015	-0.142			
195	1013.1136	-0.196	281	1270.4029	-0.196
196	1013.1143	-0.211	282	1270.4078	-0.210
197	1013.1230	-0.140	283	1270.4090	-0.207
198	1013.1244	-0.160	284	1270.4113	-0.210
199	1013.1305	-0.184	285	1270.4123	-0.186
200	1013.1330	-0.183	286	1270.4252	-0.197
			287	1270.4261	-0.190
201	1013.1622	-0.140	288	1270.4272	-0.183
202	1013.1640	-0.142	289	1270.4585	-0.194
203	1013.1737	-0.204	290	1270.4345	-0.191
204	1013.1751	-0.184	291	1270.4354	-0.184
205	1014.0889	0.122	292	1270.4370	-0.164
206	1014.0896	0.138	293	1270.4388	-0.176
207	1014.1003	0.194	294	1270.4449	-0.135
208	1014.1010	0.209	295	1270.4456	-0.192
209	1014.1093	0.309	296	1270.4518	-0.170
210	1014.1099	0.317	297	1270.4576	-0.198
211	1014.1197	0.419	298	1270.4636	-0.173
212	1014.1201	0.449	299	1270.4726	-0.197
213	1016.0955	-0.113	300	1270.4735	-0.200
214	1016.0969	-0.115			
215	1016.1044	-0.059	301	1270.4811	-0.169
216	1016.1049	-0.074	302	1270.4818	-0.172
217	1262.2092	-0.180	303	1270.4890	-0.129
218	1262.2181	-0.176	304	1270.4897	-0.164
219	1262.2301	-0.195	305	1274.1885	-0.179
220	1262.2577	-0.232	306	1274.1904	-0.157
			307	1274.2001	-0.147
221	1262.2630	-0.206	308	1274.2008	-0.143
222	1262.2716	-0.191	309	1274.2140	-0.173
223	1262.2796	-0.203	310	1274.2147	-0.173
224	1262.2859	-0.170	311	1274.2268	-0.200
225	1262.2889	-0.219	312	1274.2275	-0.179
226	1269.3676	-0.281	313	1274.2396	-0.172
227	1269.3996	-0.202	314	1274.2407	-0.166
228	1269.4079	-0.173	315	1274.2613	-0.173
229	1269.4155	-0.198	316	1274.2623	-0.152
230	1269.4225	-0.195	317	1274.2772	-0.167
231	1269.4287	-0.232	318	1274.2786	-0.146
232	1269.4371	-0.187	319	1275.1653	-0.145
233	1269.3530	-0.223	320	1275.1659	-0.151
234	1270.1956	-0.169			
235	1270.1961	-0.176	321	1275.1665	-0.158
236	1270.2270	-0.170	322	1275.1771	-0.136
237	1270.2279	-0.169	323	1275.1778	-0.119
238	1270.2333	-0.189	324	1275.1890	-0.091
239	1270.2342	-0.179	325	1275.1897	-0.078
240	1270.2390	-0.200	326	1275.1968	-0.092
			327	1275.2005	-0.037
241	1270.2430	-0.168	328	1275.2013	-0.026
242	1270.2472	-0.197	329	1275.2165	0.076
243	1270.2474	-0.163	330	1275.2172	0.070
244	1270.2482	-0.169	331	1275.2271	0.149
245	1270.2529	-0.173	332	1275.2279	0.154
246	1270.2536	-0.182	333	1275.2375	0.221
247	1270.2589	-0.185	334	1275.2382	0.234
248	1270.2601	-0.183	335	1275.2494	0.300
249	1270.2643	-0.194	336	1275.2501	0.312
250	1270.2654	-0.180	337	1275.2508	0.314
251	1270.2707	-0.169	338	1275.2608	0.413
252	1270.2714	-0.175	339	1275.2614	0.440
253	1270.2764	-0.186	340	1275.2709	0.494
254	1270.2772	-0.188			
255	1270.2821	-0.190	341	1275.2716	0.512
256	1270.2828	-0.168	342	1275.2809	0.593
257	1270.2881	-0.170	343	1275.2821	0.593
258	1270.2888	-0.182	344	1275.2963	0.612
259	1270.2953	-0.203	345	1275.2975	0.598
260	1270.2960	-0.203	346	1275.2985	0.612
			347	1275.2997	0.649
			348	1275.3002	0.651

Table 5b - continued

S.No.	JD(hel) 2440000+	Δm_b	S.No.	JD(hel) 2440000+	Δm_b
349	1275.3614	0.000	437	1349.2818	0.309
350	1275.3619	0.658	438	1349.2920	0.432
351	1275.3288	0.013	439	1349.2927	0.422
352	1275.3293	0.622	44C	1349.3036	0.536
353	1275.3352	0.568			
354	1275.3399	0.565			
355	1275.3457	0.477	441	1349.3042	0.531
356	1275.3462	0.462	442	1687.1124	-0.190
357	1275.3582	0.413	443	1687.1131	-0.191
358	1275.3591	0.419	444	1687.1309	-0.199
359	1275.3684	0.317	445	1687.1316	-0.204
36C	1275.3695	0.323	446	1687.1424	-0.198
			447	1687.1431	-0.196
			448	1687.2555	-0.217
361	1275.3790	0.246	449	1687.2565	-0.225
362	1275.3796	0.236	45C	1687.2698	-0.221
363	1275.3905	0.141	451	1687.2705	-0.217
364	1275.3912	0.154	452	1687.2806	-0.237
365	1275.4031	0.040	453	1687.2813	-0.229
366	1275.4038	0.091	454	1687.2906	-0.210
367	1275.4203	-0.053	455	1687.2913	-0.182
368	1275.4211	-0.047	456	1687.3014	-0.211
369	1275.4342	-0.121	457	1687.3021	-0.224
37C	1275.4349	-0.128	458	1687.3125	-0.204
371	1275.4514	-0.141	459	1687.3132	-0.203
372	1275.4523	-0.152	46C	1687.3220	-0.194
373	1275.4629	-0.169			
374	1275.4634	-0.158			
375	1275.4728	-0.145	461	1687.3227	-0.194
376	1275.4737	-0.150	462	1687.3373	-0.203
377	1295.1616	-0.215	463	1687.3438	-0.207
378	1295.1625	-0.220	464	1688.1072	-0.218
379	1295.1706	-0.184	465	1688.1159	-0.217
38C	1295.1714	-0.178	466	1688.1224	-0.214
			467	1688.1381	-0.196
			468	1688.1453	-0.211
381	1295.1797	-0.193	469	1688.1523	-0.207
382	1295.1803	-0.201	47C	1688.1599	-0.214
383	1295.1914	-0.210	471	1688.1702	-0.218
384	1295.1923	-0.210	472	1688.1774	-0.236
385	1295.2035	-0.236	473	1688.2402	-0.188
386	1295.2077	-0.253	474	1688.2461	-0.160
387	1295.2202	-0.244	475	1688.2520	-0.193
388	1295.2211	-0.243	476	1688.2579	-0.196
389	1295.2326	-0.249	477	1688.2641	-0.216
39C	1295.2686	-0.203	478	1688.2865	-0.184
391	1295.2691	-0.203	479	1688.2924	-0.182
392	1295.2782	-0.215	48C	1688.2980	-0.188
393	1295.2788	-0.215			
394	1295.2884	-0.208			
395	1295.2889	-0.249	481	1688.3034	-0.185
396	1295.3014	-0.216	482	1688.3090	-0.182
397	1295.3021	-0.215	483	1688.3142	-0.167
398	1295.2903	-0.208	484	1688.3201	-0.183
399	1295.3171	-0.209	485	1694.1275	-0.224
4CC	1295.3185	-0.185	486	1694.1283	-0.224
			487	1694.1369	-0.204
			488	1694.1449	-0.211
4C1	1295.3308	-0.194	489	1694.1518	-0.204
4C2	1295.3313	-0.208	49C	1694.1603	-0.198
4C3	1295.3413	-0.225	491	1694.1904	-0.205
4C4	1295.3417	-0.226	492	1694.1959	-0.210
4C5	1295.3527	-0.203	493	1694.2071	-0.203
4C6	1295.3533	-0.201	494	1694.2284	-0.208
4C7	1295.3826	-0.192	495	1694.2350	-0.218
4C8	1295.3831	-0.195	496	1694.2415	-0.231
4C9	1295.3928	-0.206	497	1694.2476	-0.184
41C	1295.3944	-0.202	498	1694.2536	-0.166
411	1295.4036	-0.205	499	1694.2592	-0.207
412	1295.4042	-0.208	5CC	1694.2647	-0.175
413	1295.4153	-0.204			
414	1295.4160	-0.195			
415	1295.4269	-0.205	5C1	1694.2706	-0.217
416	1295.4276	-0.210	5C2	1694.2766	-0.207
417	1349.1797	-0.154	5C3	1694.2849	-0.200
418	1349.1799	-0.167	5C4	1694.2911	-0.177
419	1349.1876	-0.155	5C5	1694.2973	-0.188
42C	1349.1883	-0.093	5C6	1694.3046	-0.202
			5C7	1694.3106	-0.204
			5C8	1694.3180	-0.204
421	1349.1960	-0.172	5C9	1694.3305	-0.169
422	1349.1967	-0.193	51C	1694.3372	-0.177
423	1349.2050	-0.153	511	1702.1230	-0.210
424	1349.2065	-0.144	512	1702.1237	-0.204
425	1349.2153	-0.115	513	1702.1352	-0.219
426	1349.2160	-0.119	514	1702.1656	-0.227
427	1349.2270	-0.080	515	1702.1742	-0.217
428	1349.2351	-0.040	516	1702.1839	-0.211
429	1349.2360	-0.023	517	1702.2034	-0.220
43C	1349.2489	0.046	518	1702.2102	-0.214
431	1349.2469	0.053	519	1702.2169	-0.234
432	1349.2591	0.133	52C	1702.2243	-0.200
433	1349.2601	0.147			
434	1349.2707	0.232			
435	1349.2714	0.229	521	1702.2368	-0.210
436	1349.2809	0.315	522	1702.2426	-0.195

Table 5b - continued

S.No.	JD(hel) 2440000+	Δm_b
523	1702.4604	-0.149
524	1702.2665	-0.196
525	1702.2730	-0.190
526	1702.2788	-0.208
527	1702.2843	-0.204
528	1702.2912	-0.182
529	1702.2977	-0.212
530	1702.3048	-0.195
531	1704.2892	-0.217
532	1704.2998	-0.235
533	1704.2194	-0.140
534	1704.2260	-0.140
535	1704.2288	-0.176
536	1704.2297	-0.153
537	1704.2374	-0.184
538	1704.2381	-0.176
539	1704.2458	-0.163
540	1704.2614	-0.176
541	1704.2791	-0.184
542	1704.2846	-0.189
543	1704.2927	-0.191
544	1704.2982	-0.133
545	1704.3041	-0.129
546	1704.3100	-0.191
547	1704.3173	-0.189
548	1705.1168	0.587
549	1705.1175	0.578
550	1705.1253	0.625
551	1705.1548	0.276
552	1705.1614	0.206
553	1705.1614	0.206
554	1705.1624	0.207
555	1705.1694	0.180
556	1705.1760	0.126
557	1705.1770	0.140
558	1705.1867	0.016
559	1705.1876	0.096
560	1705.1948	-0.035
561	1705.2296	-0.148
562	1705.2358	-0.192
563	1705.2569	-0.168
564	1705.2622	-0.191
565	1705.2678	-0.199
566	1705.2788	-0.174
567	1705.2837	-0.161
568	1705.2890	-0.158
569	1705.2996	-0.168
570	1705.3052	-0.143
571	1705.3105	-0.159
572	1706.0999	-0.192
573	1706.1076	-0.185
574	1706.1092	-0.204
575	1706.1174	-0.181
576	1706.1245	-0.178
577	1706.1332	-0.193
578	1706.1596	-0.169
579	1706.1664	-0.188
580	1706.1726	-0.174
581	1706.1806	-0.184
582	1706.1863	-0.198
583	1706.1917	-0.201
584	1706.1974	-0.219
585	1706.2027	-0.023
586	1706.2039	-0.013
587	1706.2139	-0.158
588	1706.2194	-0.196
589	1706.2306	-0.192
590	1706.2320	-0.219
591	1706.2375	-0.197
592	1706.2438	-0.190
593	1706.2490	-0.215
594	1706.2539	-0.241
595	1706.2588	-0.219
596	1706.2638	-0.201
597	1706.2690	-0.191
598	1706.2745	-0.221
599	1706.2796	-0.219
600	1706.2886	-0.213
601	1706.2935	-0.196
602	1706.2995	-0.214
603	1706.3041	-0.185
604	1706.0993	-0.180
605	1707.1572	0.659
606	1707.1644	0.618
607	1707.1700	0.573
608	1707.2014	0.355
609	1707.2075	0.300
610	1707.2128	0.267

S.No.	JD(hel) 2440000+	Δm_b
611	1707.2178	0.217
612	1707.2231	0.147
613	1707.2280	0.110
614	1707.2337	0.111
615	1707.1141	0.509
616	1707.1241	0.626
617	1707.1493	0.664
618	1708.1126	-0.079
619	1708.1458	-0.179
620	1708.1531	-0.159
621	1708.1607	-0.133
622	1708.1617	-0.126
623	1708.1682	-0.143
624	1708.1744	-0.171
625	1708.1804	-0.176
626	1708.1866	-0.164
627	1708.1918	-0.140
628	1708.1970	-0.149
629	1708.2022	-0.163
630	1708.2210	-0.179
631	1708.2216	-0.157
632	1708.2242	-0.173
633	1708.2308	-0.174
634	1708.2555	-0.195
635	1708.2753	-0.221
636	1708.2823	-0.173
637	1708.2871	-0.184
638	1708.2971	-0.244

Table 4

Time of Primary Minimum of HU Tauri

HD Hel	Cycle	$(O-C)_1$	$(O-C)_2$		Reference.
2400000+					
25641.300	-7603	+0.030	+0.024	PG	Strohmeier and
26005.249	-7426	+0.015	+0.008	PG	Knigge (1960)
26406.279	-7231	+0.066	+0.060	"	"
26735.269	-7071	+0.050	+0.042	"	"
26743.424	-7067	-0.022	-0.029	"	"
27039.492	-6923	-0.061	-0.068	"	"
27101.297	-6893	+0.055	+0.048	"	"
27397.346	-6749	-0.003	-0.010	"	"
28131.487	-6392	+0.040	+0.032	"	"
28931.323	-6003	-0.025	-0.032	"	"
29194.488	-5875	-0.066	-0.073	"	"
29196.541	-5874	-0.069	-0.077	"	"
34635.601	-3229	+0.080	+0.072	"	"
36597.294	-2275	+0.064	+0.055	"	"
36599.269	-2274	-0.017	-0.026	"	"
36895.449	-2130	+0.056	+0.047	"	"
36899.483	-2128	-0.023	-0.032	"	"
38733.741	-1236	+0.016	+0.007	Visual	Robinson(1965)
39169.664	-1024	+0.004	-0.005	"	" (1967)
39194.338	-1012	+0.003	-0.007	"	" (1966)
39492.501	- 867	+0.002	-0.007	"	" (1967)
40981.261	- 143	+0.002	-0.008	PE	Present Investi-
41012.113	- 128	+0.009	-0.001	"	gation
41275.310	0	0	-0.010	"	"
41707.145	+ 210	+0.012	+0.002	"	"
41984.745	+ 345	+0.012	+0.002	"	D.B.Wood -
41986.801	+ 346	+0.012	+0.002	"	Private Commu-
41990.914	+ 348	+0.012	+0.002	"	nication(1977)
41992.970	+ 349	+0.012	+0.002	"	"

Table 4 - continued

HD Hel	Cycle	$(O-C)_1$	$(O-C)_2$	Reference.
		Times of Secondary Minimum		
2441013.14	-	-	-0.002 PE	Present Investiga-
1706.13	-	-	+0.015 "	tion
1987.83	-	-	+0.002 "	D.B. Wood - Private
1989.88	-	-	0.00 "	communication
1991.94	-	-	0.00 "	"
3400.501	-	-	0.00 "	Ebersberger et al (1978)

ephemeris of HU Tau:

$$\text{Hel. Min. I} = \text{JD } 2425641.285 + 2^{d}.056288E$$

All published times of primary minima are listed in Table 6. Dr. D.B. Wood (1977) communicated four times of primary minima and three times of secondary minima from his photoelectric observations. Low weight is given for visual times of minima. A linear least squares solution of all the times of primary minima listed in Table 6 yields the following ephemeris:

$$\text{Hel. Min. I} = \text{JD } 41275.320 + 2^{d}.0562993E$$
$$\pm.005 \quad \pm \quad 13$$

The residuals $(O-C)_1$ and $(O-C)_2$ listed in Table 6 are calculated from both the old and new ephemerides respectively. A plot of the residual of the observed times of primary minima (Table 4, $(O-C)_2$) is shown in Figure 8. There are no observed times of minima during JD 2429200-2434500. The scatter in the diagram is high because of the low accuracy of photographic and visual times of minima. It appears that there is no variation in the period of HU Tau.

4.3 Light Curves

The problem which the observer of HU Tau encounters

in obtaining a complete light curve is that the period of this system is very nearly equal to two days. It is, therefore, possible to obtain a complete light curve at a single site only after several seasons of observing, and hence our light curve suffers from this defect. The heliocentric Julian day of observations are converted into orbital phases with the new ephemeris given above. The blue and yellow light curves are shown in Figure 9. These indicate asymmetry near the beginning and ending of the primary minimum. The shoulder of the light curve near the first contact is fainter than the shoulder at the fourth contact. There is an increase in brightness immediately after the primary minimum. Similar asymmetry near the first and fourth contacts was found in the light curve of U Cep (Batten 1974). Bolkadze (1956) suggested that the asymmetry of the light curve is due to the veiling of the light of the primary star by gas streams. The same explanation can be extended to HU Tau, and spectroscopic observations do support the existance of gas streams between the two stars. From the yellow light curve, the depths of primary and secondary eclipses are found to be $0^m.825$ and $0^m.06$ respectively. The secondary minima in blue and yellow are very shallow. The secondary minimum in the yellow light curve is not exactly at 0.5 phase. The scatter of the observations in the phase

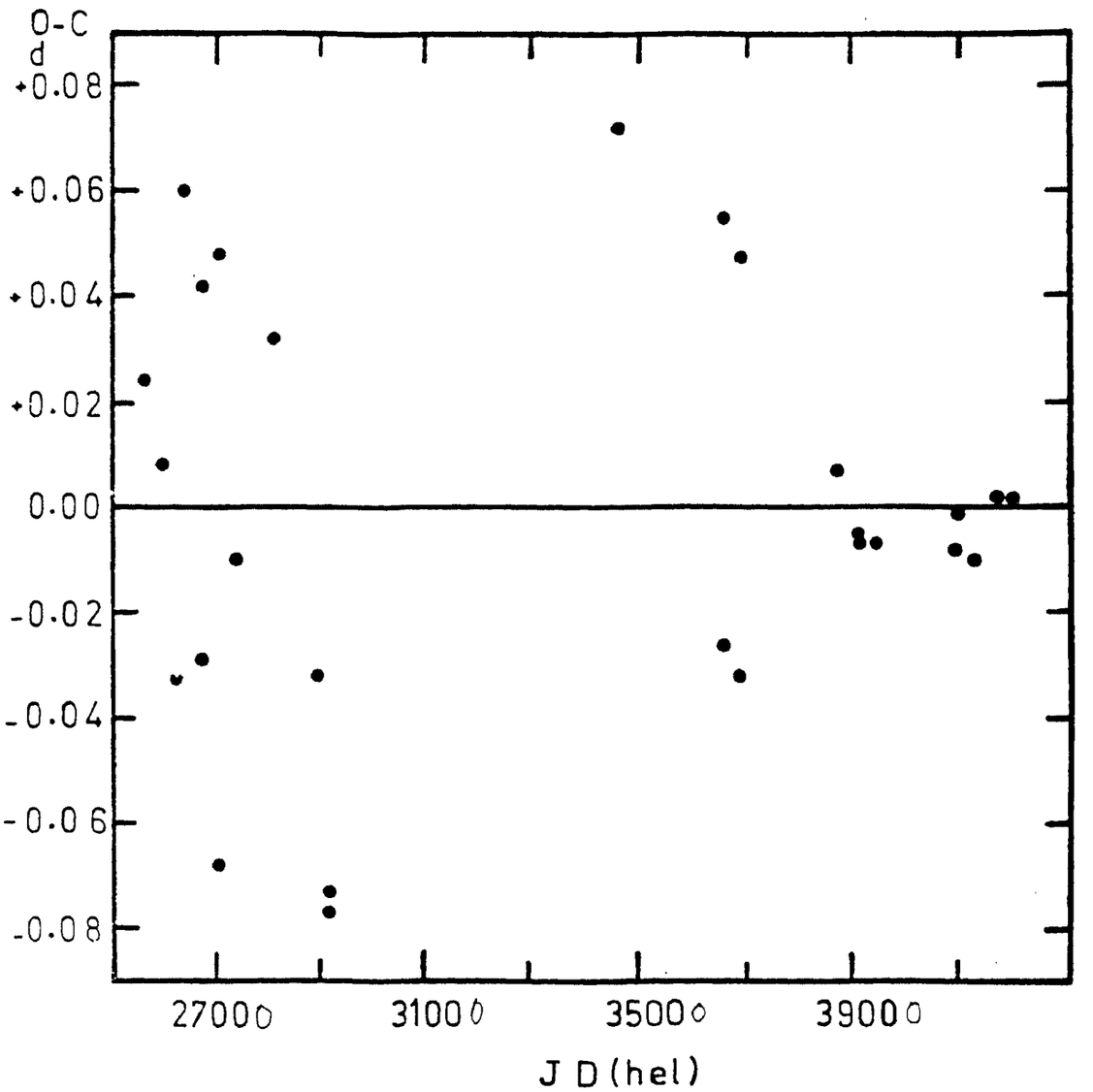

Fig.8. The plot of the residuals of the observed times of primary minima of HU Tauri

interval 0.5 - 0.75 is large and it is over and above the observational errors. Observations of standard stars and the magnitude differences between comparison star and check stars indicate the errors involved in the observations are $\pm 0^m.025$. Such variability in the light curves is not uncommon. U Cep (Batten 1974) and U Sge Cester and Pucillo (1972) and McNamara and Felts (1976) are also found to show variability from cycle to cycle.

4.4 Rectification

The rectification of the light curves was made according to the method described by Russell and Merrill (1952). To normalise the light outside eclipse to unity, a value of $-0^m.20$ and $+0^m.04$ is subtracted from the blue and yellow observations respectively. The value of external tangency $\theta_e = 28°$ was determined according to the graphical method described by Russell and Merrill (1952). Light variations between the minima were represented by the Fourier expansion:

$$= A_0 + A_1 \cos\theta + A_2 \cos 2\theta = B_1 \sin\theta + B_2 \sin 2\theta.$$

The values of the coefficients obtained by a least squares fit are given in Table 6 together with their probable errors. Coefficients of the sine terms (Table 7) were found to be very small. As the coverage of the light

Table 6

Fourier Coefficients for light outside eclipses of HU Tauri

Filter	Ao	A1	A2	B1	B2
Blue	0.9884 ± 14	-0.0116 ± 16	-0.0176 ± 23	-	-
	0.9899 ± 16	-0.0129 ± 25	-0.0178 ± 23	0.0023 ± 27	-0.0018 ± 39
Yellow	0.9871 ± 13	-0.0105 ± 14	-0.0112 ± 19	-	-
	0.9868 ± 15	-0.0125 ± 16	-0.0173 ± 15	0.0070 ± 19	0.0010 ± 28

Rectification Coefficients

	Blue	Yellow
Co	0.0115	0.0083
C1	0.0116	0.0105
C2	0.0038	0.0028
Z	0.04	0.04

curves outside eclipses is fragmentary and because of the insignificant sine terms, a second solution was obtained including only cosine terms and these are also listed in Table 7, and are used to rectify the light curves. For each colour the C coefficients were calculated from the expressions (Russell and Merrill 1952)

$$C_0 = 3C_2 = 0.09 \sin^2 \theta_2$$
$$C_1 = -A_1$$

Rectification of the light in each colour in eclipse was performed with the equation

$$l_{rec} = \frac{l + C_0 + C_1 \cos\theta + C_2 \cos 2\theta}{A_0 + C_0 - (A_2 + C_2)\cos 2\theta}$$

and rectification for phase with

$$\sin^2 \frac{\theta'}{2} = \frac{\sin^2 \frac{\theta}{2}}{1 - 2\cos^2 \theta}$$

where

$$N_2 = \frac{-(A_2 - C_2)}{A_0 - C_0 - A_2 + C_2}$$

x and y are limb and gravity darkening coefficients respectively.

Here $$N = \frac{(15+x)(1+y)}{15-5x}$$

$N = 2.2$ when $x = 0.4$

The limb darkening coefficient x = 0.4 is used which is appropriate for the spectral type of HU Tau and wavelengths of observations. After obtaining the preliminary solution the C coefficients were recomputed from the A1 coefficients and relative luminous efficiencies E_c and E_h of the cool and hot components respectively. To do this the luminous efficiency ratio $\frac{E_c}{E_h}$ is obtained by solving the quadratic equation

$$\left(\frac{E_c}{E_h}\right)^2 - 2.5 A_1 \cos i \left(\frac{E_c}{E_h}\right) - \frac{1}{4}\left(\frac{r_c}{r_h}\right)^2 = 0$$

The final rectification coefficients are given in Table 7.

4.5 Solution of the light curves

Before proceeding with the solution itself, the character of the eclipses needs to be determined. From the observed light curves (Figure 9) it is clear that the eclipses are partial and the shape of the light curve is similar to that of Algol's light curve. In a majority of the Algol systems the primary minimum is an occultation

eclipse. From the χ functions (Merrill 1950) it was verified from the rectified data, with the fact that $\chi^{tr}(n = 0.8) < \chi^{oc}(n = 0.8)$ and $\chi^{tr}(n = 0.2) > \chi^{oc}(n = 0.2)$ that the primary minimum is an occultation eclipse. The depth and shape relations were obtained for each minimum from the rectified yellow and blue light curves. No unique intersection of depth relation with shape relation was found. Therefore, using the depth relation a series of theoretical light curves in yellow and blue are computed. In the depth relation

$$\chi_0^{oc} = (1 - l_0^{oc}) + \frac{1 - l_0^{tr}}{q_0}$$

the parameter q_0 is also functionally related to the ratio of radii, k, and to the geometric depth at mid-eclipse, p_0. Using the tabulated values of $k(x, q_0, p_0)$ (Merrill 1950) values of k can be estimated. Using the k, χ_0^{oc} and α_0^{tr} found from the depth relation, a series of theoretical light curves in yellow and blue were computed with k ranging from 0.70 to 0.90 with an interval of 0.025. After obtaining a reasonable agreement between the rectified and computed light curves the rectified eclipse depth and the value of external

tangency were slightly adjusted and the above-mentioned procedure of light curve computation was repeated. The secondary minimum in the blue light curve is very shallow and the intrinsic scatter of the observations is large in the blue light curve in the phase interval 0.5 - 0.75. D.B. Wood (1977, private communication) from his unpublished photoelectric observations indicated that in the ultraviolet (Stromgren u) the light curve is quite elevated around secondary eclipse. Because of the scatter and shallow secondary minimum in the blue light curve, it is hard to estimate the rectified depth. Therefore, using the rectified depth of the primary minimum in blue and α_0 and q_0 obtained from the solution of the yellow light curve, the rectified depth $(1 - l_0^{tr})$ of the secondary minimum in blue is estimated and is used in the light curve computation. The final geometric and photometric elements, which represent the rectified light curves satisfactorily, are given in Table 8. The computed yellow and blue light curves with the elements given in Table 8 and the rectified observations (the descending branch observations are folded on to the ascending branch) during the primary minimum are shown in Figure 10. The fractional luminosities of the components in yellow and blue after correcting for reflection effect are also given in Table 8. These have been computed using

Table 7

Geometrical and Photometric elements of HU Tauri

Period	P	$2^d.0562993$
External tangency	θ_e	27°
Orbital inclination	i	77°.1
Fractional radius of the smaller star	r_s	0.221
Fractional radius of the larger star	r_g	0.284
Ratio of the radii	k	0.778
Limb darkening coefficient (assumed)	x	0.4
	α_0	0.583

	Blue	Yellow
$(1-l_0)^p$	0.520	0.513
$(1-l_0)^s$	0.038	0.042
L_s	0.891	0.880
L_g	0.109	0.120
L^*_s	0.919	0.906
L^*_g	0.081	0.094
J^*_g/J^*_s	0.053	0.063

the following expressions

$$L'_g = L_g - 0.8 L_s r_g^2 (E_g / E_s)$$

$$L'_s = L_s - 0.8 L_g r_s^2 (E_s / E_g)$$

The E - coefficients are the luminous efficiencies already defined above. The fractional luminosities given in Table 8 are

$$L''_g = L'_g / (L'_g + L'_s)$$

$$L''_s = L'_s / (L'_g + L'_s)$$

The ratio of the average surface brightness J''_g / J''_s is computed using the expression

$$J''_g / J''_s = L''_g r_s^2 / L''_s r_g^2$$

The provisional elements communicated by D.B. Wood (1977, private communication) are $i = 77.^{\circ}9$ and the fractional radii $r_s = 0.206$ and $r_g = 0.267$. These elements agree fairly well with the present solution. However, D.B. Wood's preliminary solution is based on an incompletely observed primary minimum.

Computations were also made assuming that the primary minimum is due to a transit eclipse. The complete disagreement between the computed and observed curves shows that the primary minimum is not a transit eclipse.

In the next section an analysis of the radial velocity observations of HU Tau are discussed and combining the spectroscopic orbital elements and photometric elements absolute dimensions of the system are determined.

4.6 Spectroscopic orbit of HU Tau

Spectroscopic observations of HU Tauri in the blue and in the H_α region were made using the 102cm Kavalur reflector and cassegrain spectrograph during the period, January 1974 to December 1974. All the spectra were widened to 400 microns and with a projected slit width of 20 microns. A few spectra in the H_α region were widened to 800 microns. The blue spectra were obtained on Eastman Kodak 103a-O and IIa-O (baked and unbaked) plates. The spectra in the H_α region were obtained on Eastman Kodak 098-02, 103a-E and 103a-F plates. Typical exposure times were 30 to 60 minutes for blue plates and 90 minute for spectra in the H_α region.

Fifty spectrograms in the blue region (25Å/mm at H_γ) and twenty spectrograms in the H_α region (17Å/mm) of

HU Tau were obtained. Some of the above spectra were exposed for radial velocity determination and a few for spectrophotometry. In all thirtyeight spectra were used for the study of radial velocities of the primary component. All spectra were measured with a Zeiss Abbe comparator. The blue spectra cover a wavelength range from 3700-4500. The wavelengths used for radial velocity measurement are H_γ, H_δ, H_ϵ and H_β. The HeI (4026.2A) and SiII (4128.0A) lines were found to be very weak and are not included in the measurement. The successive columns in Table 9 give the plate number, emulsion, the heliocentric Julian day of observation at mid-exposure, the phase computed using the ephemeris given in Section 4.2, the measured radial velocity reduced to the sun, and the residual computed from the elements given in Table 11.

Several radial velocity standard stars were observed during the observations of HU Tau. Measures of these plates provided the systematic correction applied on all velocities of HU Tauri. Velocities given in Tables 9 and 10 are on the standard system.

Orbital elements

The preliminary elements were obtained by the Lehman-Filhes method are:

V_o = -16 km/sec

K = 62 km/sec

e = 0.16

ω = 325°.5

T_o = JD 2441276.8004

and the standard deviation computed from the sum of the squares of the residuals is found to be ± 12.6 km/sec. The preliminary solution indicates that the orbit is eccentric. Mammano et al. (1967) determined the spectroscopic orbital elements of HU Tau. Their solution is based on the velocities determined from 53 spectra (42Å/mm at Hγ). The observations and the solution of Mammano et al. (1967) clearly indicate that the orbit is circular.

Solution 1

Because of the observational evidence for the presence of gaseous stream in the system (see Figures 2 and 12) the orbital eccentricity obtained from the preliminary solution is considered to be spurious. The present radial velocity determinations seem to be distorted by the gaseous matter in the system. Because of clear evidence for a circular orbit from the investigation of Mammano et al. (1967) no attempt is made to solve for an eccentric orbit. Therefore, making the orbital eccentricity e = 0

in the equation for the velocities we have

$$V_2 = V_0 + K\cos(\nu + \omega)$$

using the values of V_0 and K obtained from the preliminary solution the residuals in the velocities are computed and the differential corrections in ΔV_0 and ΔK are obtained from a least squares solution using the equation

$$\Delta V_2 = \Delta V_0 + \Delta K\cos(\nu + \omega)$$

Solution obtained in this manner is given in Table 11 and the computed velocity curve is shown in Figure 11a. The values of V_0 and K obtained from this solution are found to differ from those determined by Mammano et al. (1967).

Solution 2

From Figure 11a, it is clear that the observed velocities in the phase interval 0.56 - 0.68 deviate systematically from the computed curve. For this reason those five points were excluded and a fresh solution was carried out with e = 0 and the resulting orbital elements are given in Table 11 and the computed curve is shown in Figure 11b.

Table 8

Radial Velocities of HU Tauri

Plate No.	Emulsion	JD(hel)	Phase	Radial Velocity km/sec	(O-C)1 km/sec	(O-C)2 km/sec	(O-C)3 km/sec.
1.	2.	3.	4.	5.	6.	7.	8.
		2442000+					
3142	IIa-0	404.238	0.0042	-17	- 7	-10	-13
3026	"	363.309	.1054	-41	+ 4	+ 3	- 1
3027	"	363.359	.1295	-62	-10	-11	-14
3006	103a-0	361.312	.1341	-78	-25	-26	-29
3111	IIa-0	384.131	.2313	-67	+ 1	+ 0	- 2
3112	"	384.157	.2439	-59	+ 9	+ 8	+ 6
2953	"	353.327	.2512	-54	+14	+13	+11
2520	103a-0	088.097	.2668	-63	+ 5	+ 4	+ 2
3092	IIa-0	382.233	.3083	-63	+ 1	+ 0	- 2
3093	"	382.268	.3252	-58	+ 4	+ 2	0
3053	103a-0	378.206	.3502	-73	-16	-17	-20
3164	IIa-0	411.258	.4186	-24	+13	+12	+ 9
3034	"	364.243	.5598	+ 4	-10	-	-
3016	"	362.228	.5795	0	-21	-	-
2991	103a-0	360.242	.6141	+ 6	-25	-	-
2992	"	360.275	.6298	+16	-20	-	-
3019	IIa-0	362.441	.6831	+30	-17	-	-
3137	"	389.298	.7441	+54	+ 2	- 3	- 6
3100	"	383.143	.7512	+66	+14	+ 9	+ 6
3138	"	389.321	.7552	+51	- 1	- 7	- 9

Table 8 - continued

1.	2.	3.	4.	5.	6.	7.	8.
		2442000+					
3101	II-a0	383.173	0.7656	+62	+10	+ 5	+ 2
3126	"	387.323	.7838	+62	+11	+ 6	+ 3
3062	"	379.202	.8342	+40	- 4	- 8	-12
3063	"	379.241	.8528	+42	+ 2	+ 2	- 6
3143	"	408.086	.8759	+43	+ 9	+ 5	+ 1
3153	"	410.143	.8762	+21	-13	-17	-21
		Radial Velocities of HU Tauri derived from H_α line					
3005	103a-E	361.251	.1044	-30	-17	+13	+11
3113	"	384.199	.2642	-67	+ 1	0	- 2
2971	098.02	355.490	.3030	-63	+ 2	1	+ 1
2382	"	051.164	.3056	-60	+ 5	3	+ 1
2396	"	053.225	.3081	-64	+ 0	- 1	- 3
2494	"	086.143	.3165	-68	- 5	- 6	- 8
3122	103a-E	387.132	.6909	+45	- 3	- 8	-11
2995	"	360.426	.7035	+70	-21	- 6	+12
2431	098.02	060.272	.7349	+52	+ 0	- 5	- 8
2926	"	350.319	.7884	+68	+18	+13	+10
2403	"	054.268	.8153	+46	- 1	- 6	- 9
3105	103a-E	383.315	.8346	+56	+12	+ 8	+ 4

Table 9

Velocities derived from the component of H_α line

Plate No.	Emulsion	JD(hel)	Phase	Velocity (km/sec)
		2442000+		
3008	098-02	361.437	0.1949	-
3113	103-aE	384.199	.2642	+273
2935	098-02	351.324	.2769	+243
2382	"	051.164	.3056	+219
2396	"	053.225	.3081	+240
2494	"	086.143	.3165	+223
3017	103-aF	362.306	.6177	-
2431	098-02	060.272	.7349	-
2926	"	350.319	.7884	-
2403	"	054.268	.8153	-208

Solution 3

The velocities determined by Mammano et al. (1967) and the velocities determined in the present investigation are combined except those in the phase interval 0.56 - 0.68 and a least squares solution was made for differential corrections ΔV_o and ΔK. The final elements are listed in Table 11 and the computed curve is shown in Figure 11c. The standard deviation is found to be 9.6 km/sec. The residuals computed with the orbital elements obtained from Solution 1, Solution 2, and Solution 3 are given in Table 9 under $(O-C)_1$, $(O-C)_2$ and $(O-C)_3$ respectively.

Why the velocities in the phase interval 0.56 - 0.68 are systematically off, is not clear ? Standard star velocities determined from the observations made during the same period do not differ significantly from the determinations made during the rest of the observing period. The blue spectrogram number 2991 and the H_γ region spectrogram number 2995 were obtained on the same night with the same spectrograph. The former spectrum is at 0.6141 phase and the later is at 0.7035 phase. The velocity determined from H_α region spectrogram (No.2995) agrees fairly well the general trend of the velocity variation at that phase, whereas the velocity determined

Table 10

Spectroscopic Orbital elements of HU Tauri

		Solution 1	Solution 2	Mammano et al(1967)	Solution 3
Period (days)	P	2.0562993	2.0562993	2.056297	2.0562993
Systemic Velocity (km/sec)	V_o	-8.1 ±2.0	-5.0±1.7	-2.3±1.3	-2.7±1.0
Semi Amplitude of the Velocity curve (km/sec)	K	60.0±2.3	62.3±2.0	65.4±1.3	63.0±1.3
Orbital eccentricity	e	0.0	0.0	0.0	0.0
Epoch of mean longitude	T_o	-	-	38805.169±.009	41276.862
Semi major axis (km)	a sini	-	-	1.85×10^6	1.7814×10^6
Mass function ($m_\odot$)	f(m)	-	-	0.0597	0.0535

from the blue spectrogram (No.2991) is off from the general trend of velocity variation at that phase. Thus the systematic deviation of velocities in the phase interval 0.56 - 0.68 is intrinsic. The plausible explanation that can be offered in view of the evidence for circumstellar matter is that it is distorting the line profile in the phase interval 0.56 - 0.68.

4.7 The H_α line

The velocities of the primary component determined from the H_α absorption line are also given in Table 9. These velocities were also used in the orbit computation. A spectrogram (No.2382) obtained on 3rd January 1974 shows a violet shifted broad emission feature. The peak velocity of the emission feature is found to be -600 km/sec. This spectrogram was obtained on Eastman Kodak 098-02 emulsion like the rest of the H_α plates. A few spectra in the H_α region were obtained on 103a-E and 103a-F emulsions. The spectrogram of 3rd January is well exposed for spectrophotometry and it is widened to 800 microns. The exposure time is 89 minutes. The violet shifted emission feature extends very much into the violet wing of the H_α line. This emission feature is absent on a plate taken immediately after one orbital period. This

indicates that the emission is subject to transient temporal changes. Such variations in intensity from cycle to cycle have been found in RW Tau (Joy 1947) and U Cep (Batten 1974 and Batten et al. 1975). The large negative velocity derived from the emission feature indicates that the material is being ejected from the system at a high velocity. Another possibility is that the B9V component possessed a transient disk which is expanding and from which some matter has probably left the system. The same spectrogram taken on 3rd January 1974 shows absorption like feature towards the red side of the H_α absorption core. This can be interpreted in two ways. Either we are seeing the H_α absorption line of the secondary, or the sharp emission feature due to the gaseous stream which is falling on the red edge of H_α line is creating an impression of an absorption line. The magnitude difference between the two components from the solution of yellow light curve is found to be $2^m.26$ and, therefore, it is unlikely that we are able to see the secondary components H_α absorption. This feature is seen on several H_α plates while on some of the spectra, it is completely absent. The H_α spectrum obtained on 29th October 1974 (plate No.2926, Phase ~.7784), has an asymmetric profile but there is no evidence for the presence of absorption-like feature on either wings of H_α, whereas

the spectrum obtained on 6th January 1974 (Plate No.2403, phase 0.8153) shows clearly that this absorption like feature is violet shifted with respect to the H_α absorption. From the above discussion, it is evident that we are not seeing the H_α absorption line of the secondary component. The interpretation is that the emission due to the gaseous stream between the two components is filling in the wings of H_α line at quadratures. The asymmetry of the H_α density profiles and their variation from cycle to cycle and the violet shifted flare like event noticed on the 3rd January 1974 (plate No.2382) give ample evidence for the presence of gas streams between the two components. No emission was detected on the plates taken during the minimum light of the primary eclipse. No sodium lines were found on the spectra taken in that region. The H_α line at phase 0.6177 is found to be broad and shallow and around the same phase interval the velocities are systematically off.

Struve and Sahade (1957) found emission in the spectrum of Algol. This emission was observed at quadratures and is a faint, broad band bordering the red edge of H_α and H_β. Later Struve, Sahade and Huang (1957) reported that there might be emission between the two components of H_α in the spectrum of U CrB. Emission at quadratures and apparent line doubling was

also noticed in the spectrum of U Cep (Batten 1974, Batten and Laskarides 1969). They have suggested that the apparent doubling of hydrogen lines is due to partial filling of the absorption line by emission originating in the gaseous stream that flows from the cooler star to the hotter star. Batten (1974) found the equivalent width of the hydrogen lines to be less when they are seen as double than at other phases. Similar variation was found photometrically for the intensity of H_α in the spectrum of Algol by Andrews (1967) which he ascribed to emission partly filling up the line. Batten (1974) found it difficult to interpret the doubling of hydrogen lines in U Cep. He had found that the line doubling in U Cep is not only noticed for H_α, but for all other hydrogen lines. Batten found that the velocities determined from the hydrogen line components agree with the expected orbital velocity of the U Cep secondary.

The velocities determined from the H_α component of HU Tau spectra are listed in Table 10 and they seem to agree with the expected radial velocity amplitude of the secondary component!?

4.8 Absolute domensions of HU Tau

Combining the photometric elements (Table 8) and the spectroscopic orbital elements (Solution 3 Table 11)

masses and dimensions of the components of HU Tau are estimated.

The relation between Roche lobe radius and mass ratio is

$$r_1 = A(0.38 + 0.2 \log \frac{m_1}{m_2})$$

where A is the separation between the centers of the two components with masses m_1 and m_2 respectively. r_1 is the Roche-lobe radius for the star with mass m_1. Assuming that the secondary component has filled the Roche lobe the mass computed from the above equation is found to be $m_2/m_1 = 0.33$. The spectral type of the primary component of HU Tau is B9V. The mass of a B9V star is $4M_\odot$ (Allen 1973). Using the mass ratio $m_2/m_1 = 0.33$ and $m_1 = 4M_\odot$ the mass of the secondary is found to be 1.2 $M_\odot$. The masses obtained from the mass function, according to the method of Kopal (1959) are found to be $m_1 = 4.3\ M_\odot$ and $m_2 = 1.2\ M_\odot$ and are also consistent with the above values. If we accept the velocities determined from the H_α absorption component to represent the orbital motion of the secondary component is found to be 234 km/sec, and the mass ratio $m_2/m_1 = K_1/K_2 = 0.27$, with $m_1 = 4.8\ M_\odot$ and $m_2 = 1.3\ M_\odot$. Surprisingly these values are consist with the masses determined from the above mentioned two methods. The

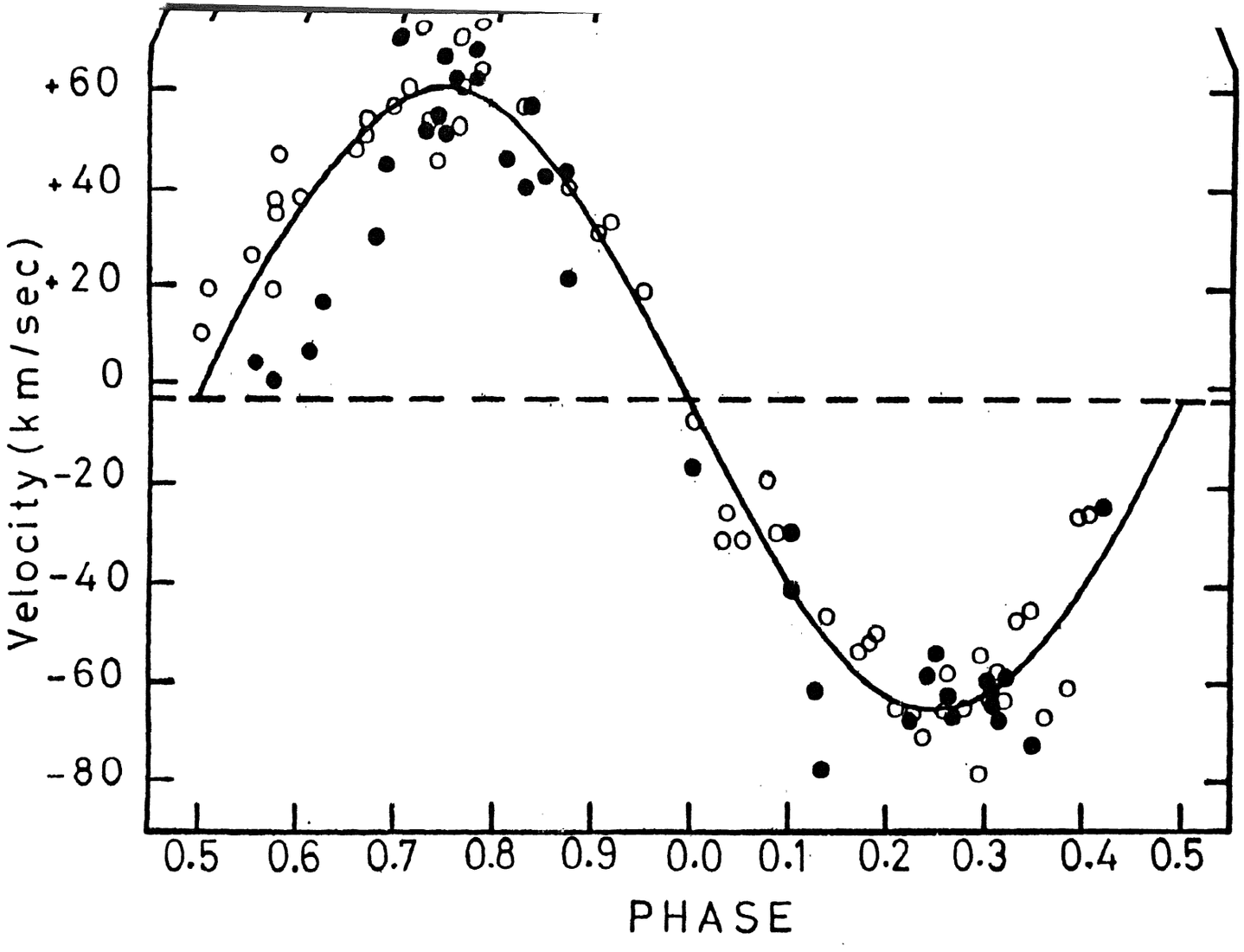

Radial velocity curve of HU Tauri

Fig.6c. Open circles denote the velocities determined by Mammano et al.(1967) and filled circles represent the velocities listed in Table 8.

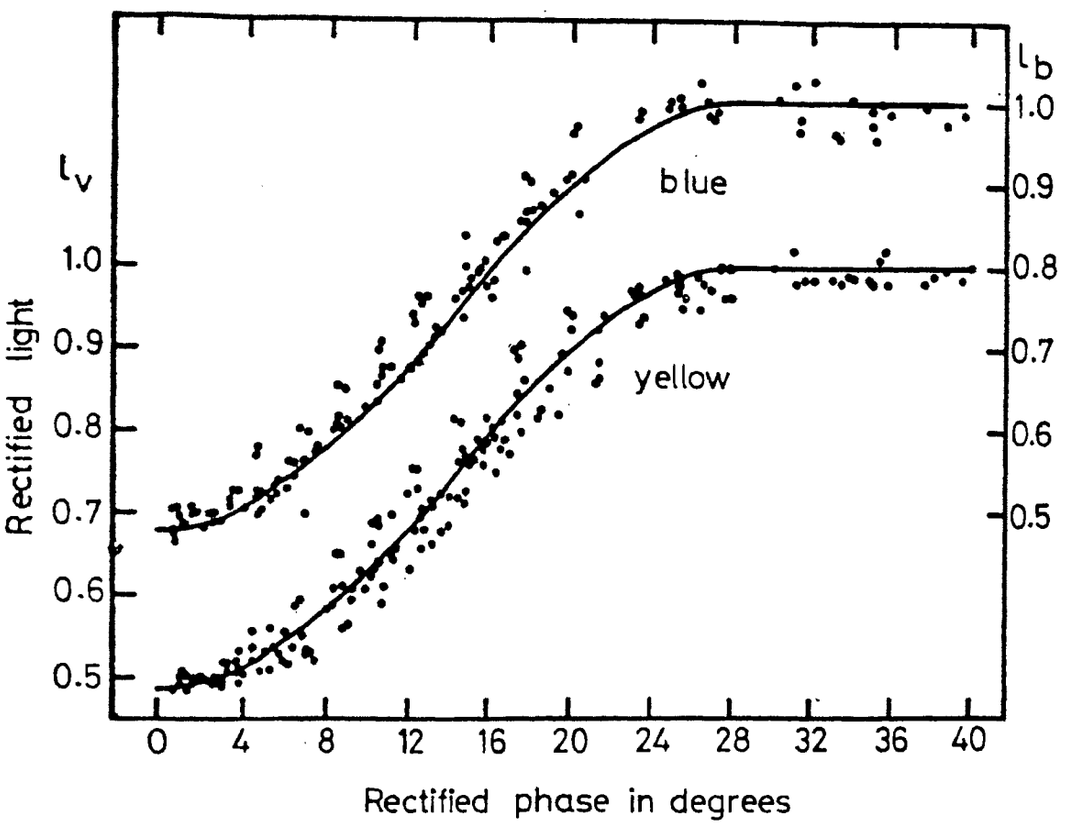

Fig.10. Rectified primary eclipse of HU Tauri. The solid curves are based on the photometric elements listed in Table 7.

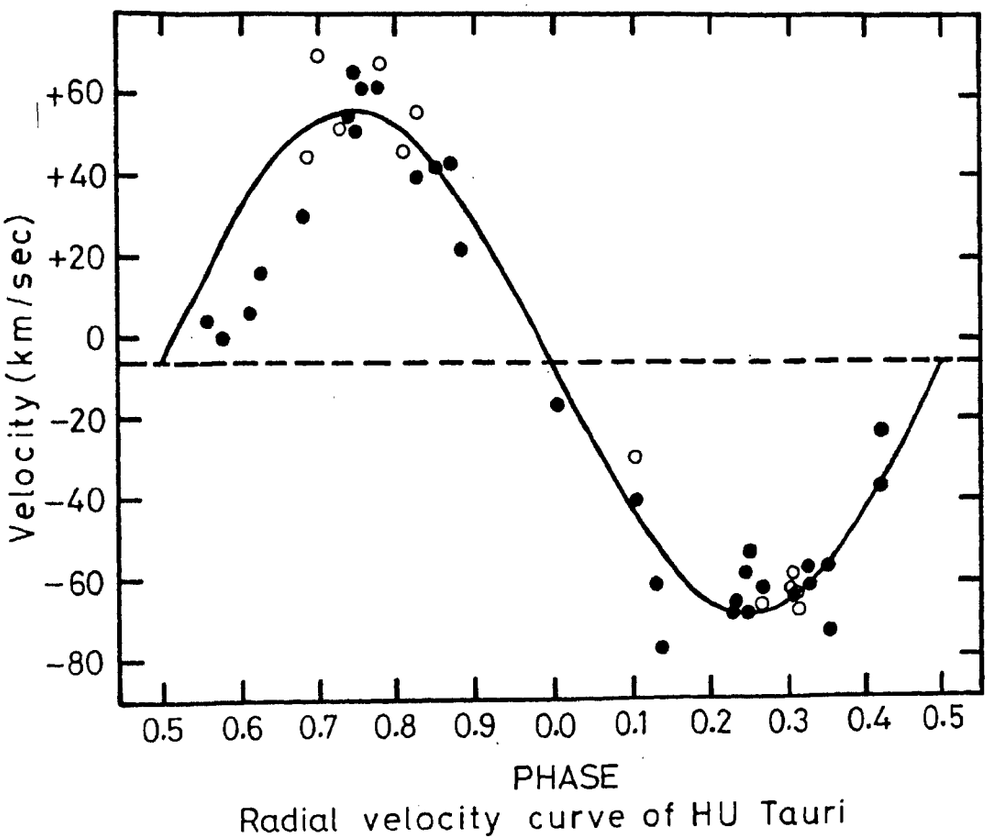

Fig.11b. Open circles denote the velocities determined from Hα line Filled circles denote the velocities determined from lines shortward of 4400 A (velocities in the phase interval 0.56-0.68 are not included in the solution).

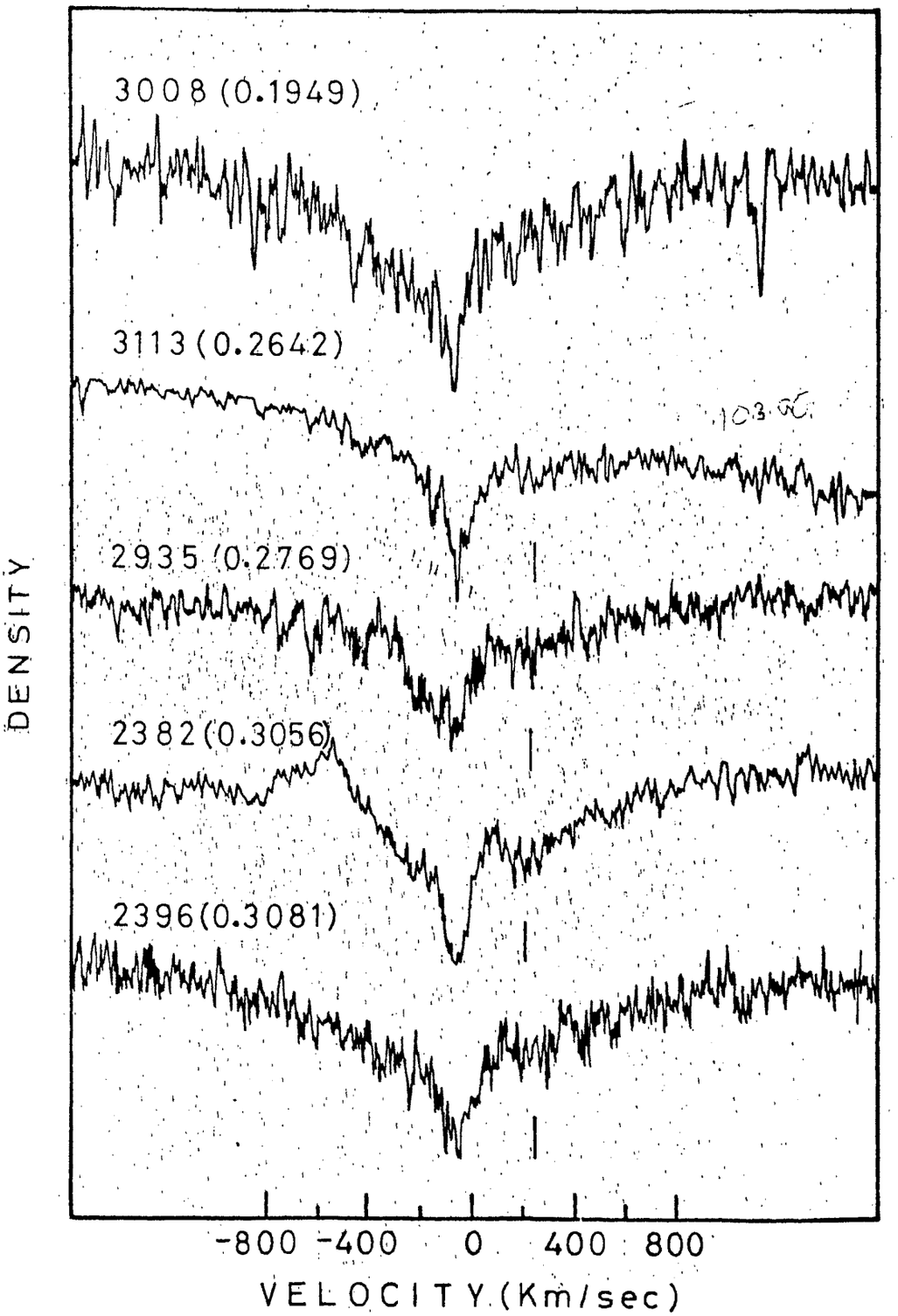

Fig.7a. Microphotometer tracings of the region of Hα. The zero of the velocity scale is the rest postion of Hα. Violet is at the left. (See Table 9)

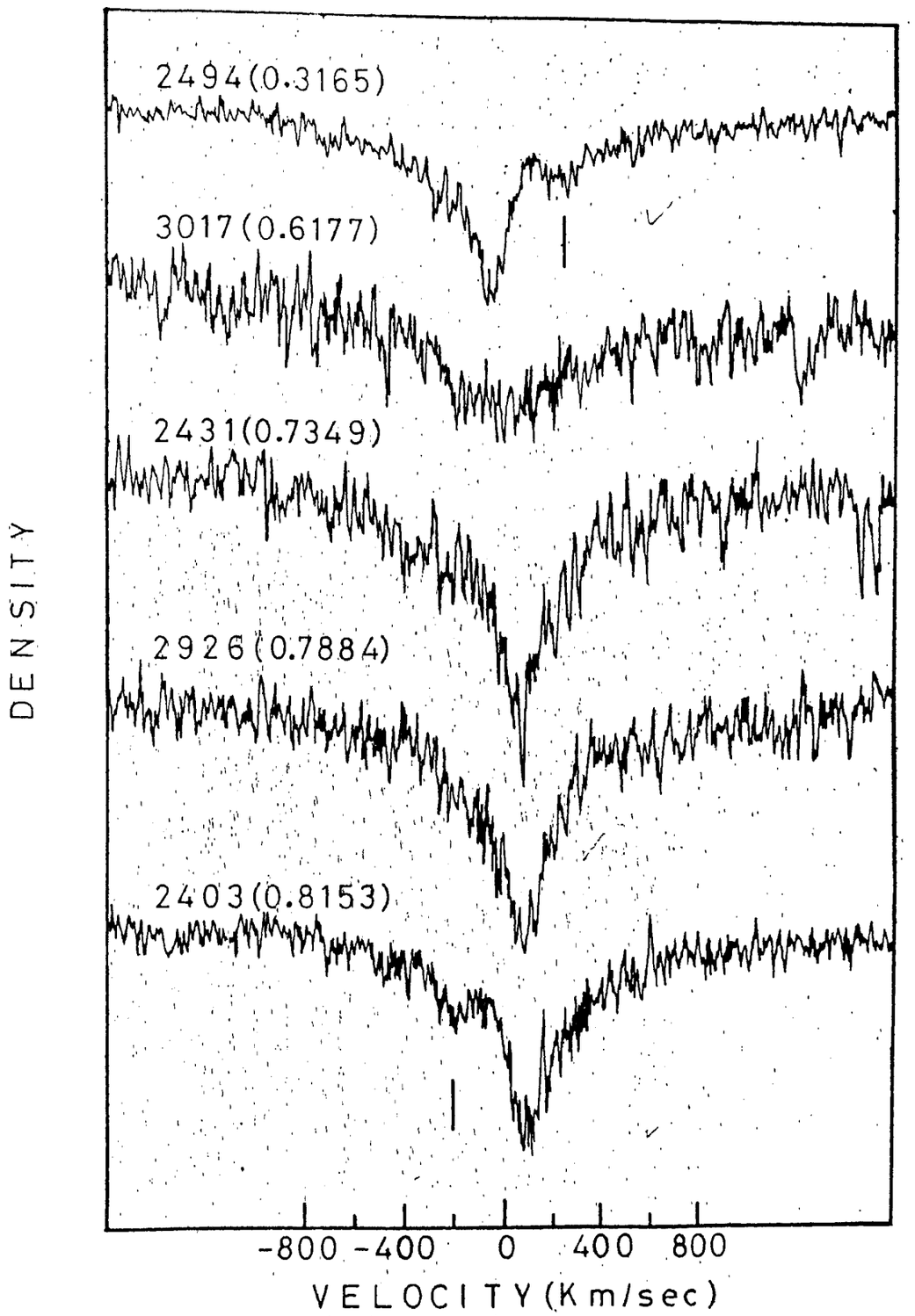

Fig.7 b. Microphotometer tracings of the region of Hα. The zero of the velocity scale is the rest position of Hα. Violet is at the left.

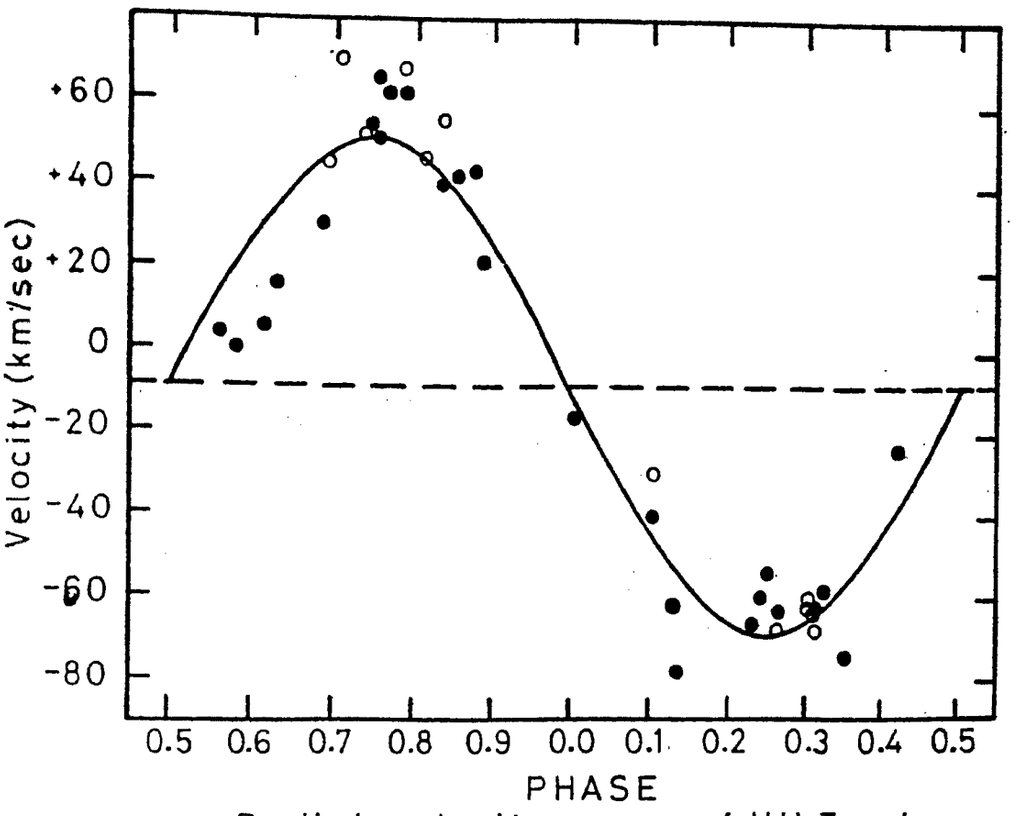

Radial velocity curve of HU Tauri

Fig. 1a. Open circles denote the velocities determined from Hα line. Filled circles denote the velocities determined from lines shortward of 4400A.

Table 11

Spectroscopic orbital elements of HU Tauri

V_o	-2.7 km/sec
K_1	63.0 km/sec
K_2	234.0 km/sec
K_1/K_2	0.27
e	0.0
$a_1 \sin i$	1.781×10^6 km
$a_2 \sin i$	6.622×10^6 km
$m_1 \sin^3 i$	4.42 $M_\odot$
$m_2 \sin^3 i$	1.19 $M_\odot$

Table 12

Masses and dimensions of the components of HU Tauri

	HU Tau		Algol		δ Lib	
	Primary	Secondary	Primary	Secondary	Primary	Secondary
Period (days)	2.056		2.867		2.327	
Spectral type	B8V		B8V	G7	B9.5V	G8
Mass Ratio	0.279		0.217		0.592	
Separation	12.45		14.0		13.82	
Mass (m_0)	4.83	1.3	3.7	0.81	4.9	1.7
Radius (R_0)	2.7	3.54	3.08	3.23	4.1	4.2
Roche Radius (R_0)	6.1 5.9	~~3.3~~ 3.2	7.18	3.46	6.53	3.97

final absolute dimensions of HU Tau are given in Table 13 together with the absolute dimensions of Algol and δ Lib for comparison. Algol and δ Lib now have well determined absolute dimensions Tomkin and Lambert (1978), Tomkin (1978). Comparison of the radii of the components of HU Tau with the Roche lobe radii given in Table 12 clearly indicates that the secondary component has filled its Roche lobe. Thus HU Tau is a typical Algol system with gas stream flowing from the secondary to the primary.

CHAPTER 5

SOME FUTURE NEEDS

In the earlier chapters of this thesis we have demonstrated that (1) the chemical composition of the secondaries of Algol systems U Cep and U Sge is normal and (2) that these secondaries have sizeable chromospheric emission as detected by filling in of the CaII triplet in the near infrared. This conclusion eliminates the possibility of the normally observed UV excess as due to metal deficiency of the secondary star in both systems. Other explanations for the UV excess can of course be chromospheric activity of the secondary or a contamination of the colours of the secondary by an extended envelope surrounding the hot primary and which is not completely eclipsed during the totality phase. The observations made by Batten of an outburst in U Cep, both in and out of eclipse, seem to rule out the possibility that the UV excess observed in the total light of the system stems from the chromospheric characteristics of the secondary.

It does not seem possible at this stage to comment conclusively on the last possibility mentioned above and

and thereby explain the UV excess interms of the extended envelope around the primary. Algol systems have large scale interaction between the two components that are interpreted in terms of massflow and circumstellar envelopes. A new system, added as a result of this study to the Algol family, HU Tau, demonstrates these features.

Much remains to be done in this very interesting area of research on close binary systems. The determination of masses of the secondary components in both short period and long period Algol systems, is a necessity. In making such studies one has to be careful in evaluating properly possible contributions from the gas-streams that might affect the results of the study of the velocity curve. Further analyses of such systems of different periods would be most useful, since, the luminosities for the secondaries of short period Algol systems, seems to be much in excess. A study similar to the one carried out here, using high resolution spectra during totality, especially aimed at determining CNO abundances, is one that is very important for the determination of the nature of the mass exchange experienced by the system since its formation. As technological developments progressively bring such studies within the realm of distinct possibility, it is necessary that one takes

vantage of the situation in evaluating whether studies the CNO content can be used for deciding on the olutionary scenario experienced by the system.

Our results have shown the presence of considerable romospheric emission associated with the secondary mponent. It is unfortunate that a simultaneous praisal of the intensity of this emission in the olet region with the aid of the H and K lines was not sible. A requirement for future study is obviously e intensity of such emission which can be definitely sociated with an origin from the secondary and perhaps on a study of time dependent changes of a short term long term nature, of such a chromospheric characteristic. similar approach confined to the study of the Lithium ne at 6708A, especially during totality would be most eful.

These are some of the major areas in which availability information in the form of reliable observations and sound theoretical interpretation would aid greatly our derstanding of the evolution of the Algol systems. ere is much that can be learned and which is within latively easy reach of present-day capability.

REFERENCES

Allen, C.W.	1973	Astrophysical quantities, 3rd edition, London, Athlone Press.
Andrews, P.J.	1967	Astrophys. J. 147, 1183
Bakos, G.A. and Tremko, J.	1977	J. Royal. Astron. Soc. Canada 71, 234
Baldwin, B.W	1973	Publ. Astr. Soc. Pacific, 85, 714
Bappu, M.K.V. and Sivaraman, K.R.	1971	Solar Phys. 17, 316
Bath, G.T.	1972	Astrophys. J. 173, 121
Batten, A.H.	1970	Publ. Astr. Soc. Pacific, 82, 574.
Batten, A.H.	1973a	Binary and Multiple systems of stars, Oxford, Pergamon Press, p. 201
Batten, A.H.	1973b	In Extended Atmospheres and circumstellar Matter in spectroscopic Binary systems, IAU Symp. No.51, ed. A.H. Batten (D. Reidel).
Batten, A.H.	1974	Publ. Dom. Astrophys. Obs. Victoria, 14, 191
Batten, A.H., Fisher, W.A., Baldwin, B.W. and Scarfe, C.D	1975	Nature, 253, 174
Batten, A.H. and Laskarides, P.G	1969	Publ. Astr. Soc. Pacific, 83, 149.
Bell, R.A., Erkisson, K., Gustafsson, B., and Nordlund, A	1976	Astr. and Astrophys. Suppl. 23, 37.

·erman, P. and ·all, D.S.	1973	Astr. Astrophys. 27, 249
›Rokade, R.D.	1956	Perem. Zevezdy, 11, 375
›nd, H.E	1972	Publ. Astr. Soc. Pacific, 84, 839
rukalska, R., Kucinski, S.M., Smak, J., and Stepien	1969	Acta Astron. 19, 257
udding, E and Kopal, Z.	1970	Astrophys. Space Sci. 9, 343
urbidge, E.M. and Burbidge, G.R.	1957	Astrophys. J., 126, 357
ester, B., Fedel, B., Giuricin, G., Mardirossian, F and Pucillo, M.	1977	Astr. Astrophys., 61, 469
ester, B. and Pucillo, M	1972	Mem. Soc. Astr. Ital., 43, 501
hen, K.Y. and Reuning, E.G.	1966	Astron. J. 71, 283
rawford, J.A	1955	Astrophys. J. 121, 71
ivinney, E.J., Hall, D.S. and Ward, D.H.	1970	Publ. Astr. Soc. Pacific 82, 10.
Frieboes-Conde, H and Herczeg, T.	1973	Astron. Astrophys. Suppl. 12, 1.
Giannone, P., Kohl, K., and Weigert, A.	1968	Z. Astrophys. 68, 107.
Glebocki, R., and Stawikowski, A.	1977	Acta. Astronomica 27, 225
Grant, G	1959	Astrophys. J. 129, 62

Griffin, R.F.	1968	A photometric Atlas of the spectrum of Arcturus 3600-8825A (Cambridge philosophical Society).
Griffin, R.F., and Redman, R.O.	1960	Mon. Not. R. Astr. Soc., 120, 287
Hall, D.S.	1967	Astr. J., 72, 301.
Hall, D.S., and Garrison, L.M.	1972	Publ. Astron. Soc. Pacific 84, 552.
Hall, D.S., and Walter, K	1974	Astr. and Astrophys. 37, 263
Hall, D.S. and Walter, K	1975	Astr. and Astrophys. Suppl. 19, 337
Hansen, L., and Kjaergaard, P.	1971	Astr. Astrophys. 15, 123
Joy, A.H.	1942	Publ. astr. Soc. Pacific 54, 35
Joy, A.H.	1947	Publ. astr. Soc. Pacific 59, 172
Khozov, G.V. and Minaev, N.A.	1969	Trudy Astr. Obs. Leningrad State Univ. 26, 55.
Kippenhahn, R., and Weigert, A	1967	Z. Astrophys. 65, 241
Koch, R.H.	1972	Publ. Astr., Soc. Pacific, 84, 5.
Kopal, Z.	1955	Ann. d'Astrophys., 18, 379
Kopal, Z.	1959	Close binary systems, New York, John Wiley & Sons Inc
Kreiner, J.M.	1971	Acta Astron. 21, 365
Kurucz, R.L., and Peytremann	1975	Smithsonian Astrophys. Obs. Spec. Rept. No.362.

Lauterborn, D.	1970	Astr. Astrophys. 7, 150
Mammano, A and Margoni, R.	1967	Mem. Soc. Astr. Ital., 38,459
McNamara, D.H.	1967	Astrophys. J., 149, 723
McNamara, D.H. and Feltz, K.A.	1976	Publ. Astr. Soc. Pacific, 88, 688
Merrill, J.E.	1950	Contri. Princeton Univ. Obs. No.23.
Miner, E.D.	1966	Astrophys. J., 144, 1101
Morton, D.C.	1960	Astrophys. J., 132, 146
Naftilan, S.A.	1975	Publ. Astr. Soc. Pacific 87, 321
Naftilan, S.A.	1976	Astrophys. J., 206, 785
Nadeau, D. et al.	1978	Mon. Not. R. astr. Soc., 184 523
Olson, E.C.	1974	Pub. Astron. Soc. Pacific 86, 80
Olson, E.C.	1976	Astrophys. J., 204, 141
Paczynski, B.	1967	Acta Astr. 17, 355
Paczynski, B.	1971	Ann. Rev. Astr. Astrophys., 9, 183.
Parthasarathy, M.	1972	Astrophys. Space Sci. 18, 190
Parthasarathy, M., Lambert, D.L., and Tomkin, J.	1978	Mon. Not. R. astr. Soc. (in press)
Plavec, M.	1968	Advances in Astr. Astrophys. 6 201.
Plavec, M.	1970	Publ. astr. Soc. Pacific, 82, 957.
Plavec, M.	1973	In IAU Symposium No.51, ed. A.H. Batten (Boston, Reidel)

Plavec, M., and Polidan, R.S.	1975	Nature, 253, 173.
Popper, D.M.	1973	Astrophys. J., 123, 246
Rhombs, C.G., and Fix, J.D.	1976	Astrophys. J., 209, 821
Rhombs, C.G., and Fix, J.D.	1977	Astrophys. J., 212, 446
Russell, H.N. and Merrill, J.E.	1952	Contr. Princeton Univ. Obs. No.26.
Sahade, J.	1958	Publ. Astr. Soc. Pacific, 70, 319
Sahade, J., and Wood, F.B.	1978	Interacting binary stars Pergamon Press.
Sistero, R.F.	1968	Publ. Astr. Soc. Pacific, 80, 474.
Sistero, R.F.	1971	Bull. Astr. Inst. Czechoslovakia, 22, 188.
Strohmeier, W.	1960	IAU Circ. 1706, 1960
Strohmeier, W., and Knigge, R.	1960	Veroff Bamberg V, (5), 1960
Struve, O., and Sahade, J.	1957	Publ. astr. Soc. Pacific, 69, 41.
Struve, O., and Sahade, J., & Huang, S.S.	1957	Publ. astr. Soc. Pacific, 69, 342.
Spinrad, H. and Taylor, B.J.	1969	Astrophys. J. 157, 1279
Tomkin, J.	1978	Astrophys. J., 221, 608
Tomkin, J.	1979	(Pre-print)
Tomkin, J., and Lambert, D.L.	1978	Astrophys. J. (Letters), 222, L119

Unsold, A., and Struve, O.	1949	Astrophys. J. 110, 455
Vogt, S., Tull, R.G., and Kelton, P.	1978	Appl. Optics, 17, 574.
Wallerstein	1962	Astrophys. J. Suppl. 6, 407
Williams, P.M.	1971	Mon. Not. R. astr. Soc., 153, 171.
Wilson, O.C.	1963	Astrophys. J., 138, 832
Wilson, O.C.	1976	Astrophys. J., 205, 823
Wilson, O.C. and Bappu, M.K.V.	1957	Astrophys. J., 125, 661
Wood, F.B.	1950	Astrophys. J., 112, 196
Wood, D.B.	1977	(Private Communication)
Young, A., and Koniges, A.	1977	Astrophys. J. 211, 836
Ziolkowski, J.	1969	Astrophys. Space Sci. 3, 14
Zirin, H.	1976	Astrophys. J., 208, 414